UNIVERSITY
OF TRENTO - Italy
Center for Mind/Brain Sciences

Category and Space in the Ventral Stream

PhD Dissertation

Student: Anne Schobert
Advisor: Prof. Jens Schwarzbach

Content

Thanks...

I would like to thank my supervisor Jens Schwarzbach for having taught me how to be a thorough and independent researcher. I hope I will be able to apply these values worthily.
I also thank Alfonso Caramazza for having "co-supervised" me for a while and for having shown interest in my progress.
The IT guys Antonio, Stefano, and Davide took a lot of trouble with fixing my technical issues and calming me down.
The MR team Hanna-Liisa and Claudio were usually on duty when I was scanning and did more than their duty in helping me.
I was very lucky to have a group of incredible and unique office mates and friends: Francesca (1 and 2), Andrea, Nicola, Vittorio. I enjoyed my three years of Italy especially because of them. Thank you, Michele and Francesca, for being ever-available guinea pigs!
I thank my running buddies Amy and Gerhard. There is nothing like a good run to share achievements and, more often, to relieve frustration and worries.
Carola is a good companion for sharing the hardships of the final phase of a PhD and she spent a lot of time helping me with formatting the manuscript.

The biggest bulk of help, however, has come from Nathaniel. He not only supported me emotionally and practically, but was also my main scientific correspondent. I learned a lot about my merits and shortcomings in our discussions about work and life. I deeply appreciate that he is always there for me.

Meine Eltern und mein Bruder unterstützen und ermutigen mich in allem, was ich tue. Ich bin mir sicher, eine handwerkliche Lehre hätten sie ebenso gepriesen wie eine wissenschaftliche Laufbahn. Solch ein Rückhalt ist etwas Besonderes.

1 General Introduction

Over the past few decades neuroscientists have attempted to understand the neural basis of a fascinating cognitive ability of humans: high-level face and object perception. We can recognize and discriminate between faces and objects in a fraction of a second and under a multitude of environmental factors (Grill-Spector, 2003; Tsao & Livingstone, 2008). The informational content of visual stimuli may be largely degraded or ambiguous; yet we can assess with high acuity what we see. The most intriguing insights on human perception of complex stimuli have come from cases where these abilities are dysfunctional or absent. Studies on patients have indicated how special visual face and object perception might be. Two particular visual deficits are prosopagnosia, which is the inability to recognize faces, and object agnosia, which refers to a deficit in identifying objects (Behrmann & Avidan, 2005; Moscovitch, Winocur, & Behrmann, 1997). The compelling aspect of these syndromes is that they usually occur selectively for faces and objects, respectively, without affecting the ability to recognize low-level (features or parts of more complex objects) or other types of high-level (faces or objects) stimuli (Busigny, Graf, Mayer, & Rossion, 2010; Cavina-Pratesi, Kentridge, Heywood, & Milner, 2010). With the advent of functional magnetic resonance imaging (fMRI) researchers have started to localize brain regions that appear to be the neural basis for such selective object recognition. Foremost, a region in the fusiform gyrus of the ventral temporal lobe has been found to be more activated when people looked at face pictures as compared to house, object or scrambled pictures (Kanwisher, McDermott, & Chun, 1997; Puce, Allison, Gore, & McCarthy, 1995) This area has been dubbed the fusiform face area (FFA). An area in the lateral occipital complex (LO) was found to be related to the encoding of a wide range of object stimuli (Malach et al., 1995).

Similarly, a region in the parahippocampal gyrus, the "parahippocampal place area" (PPA), is activated preferentially for pictures of houses and scenes (Epstein & Kanwisher, 1998). Additional stimulus categories that have been hypothesized to engage specific brain regions are the human body in the "extrastriate body area" (EBA), tools in the fusiform gyrus and animals in the superior and middle temporal gyri (Chao, Haxby, & Martin, 1999).

An ongoing debate concerns the question which aspects of a stimulus class are encoded by these brain regions. One theory states that object categories are encoded by specialized modules, with faces being perhaps the most "special" category (Kanwisher & Yovel, 2006). FFA is assumed to encode the high-level, semantic aspects of faces, and it does so in a highly abstract and feature-invariant manner. Similarly, other object categories are selectively encoded by specialized modules (Gauthier, 2000). Thus, according to the modular view, object categories are exclusively encoded by one specialized brain region. In contrast, another theory has been proposed which assumes that the ventral temporal cortex contains a widespread and continuous representation of information about object form (Ishai, Ungerleider, Martin, Schouten, & Haxby, 1999). Information that is most characteristic for object exemplars within a certain category clusters together and forms areas that respond maximally to that category. Importantly, this theory posits that object category is not selectively encoded by one specialized module but is instead encoded throughout the ventral stream. This controversy about specialized modules and distributed processing is addressed in chapter 2 of this thesis. An experiment is described that tests the two opposing theories about category representation with fMRI adaptation (fMRI-A), a method that assesses neural sensitivity to particular stimulus properties. The hypothesis is that, if category is encoded in highly selective modules, then these modules should be sensitive only to their preferred category. If, on the other hand, the distributed processing account is true, then

areas with maximal activation for one category should also show sensitivity, albeit to a lesser degree, to other categories. Our results indicate that FFA and PPA are maximally, but not exclusively sensitive to their respective preferred categories, and therefore favor a distributed representation of category.

Another interesting fact about object perception is that it seems to be organized along at least two different dimensions: identity and space. Again, patients with particular deficits have been the driving factor for the furthering of our understanding of these two dimensions. For example, patients suffering from object form agnosia exhibit a selective impairment in identifying an object, while their ability to act upon that object in an appropriate way remains intact (Ungerleider, Mishkin, Ingle, Goodale, & Mansfield, 1982). Curiously, the opposite pattern has been observed in patients who are affected by optic ataxia. While these patients have problems in interacting with an object, like appropriately reaching for it, they can nevertheless normally recognize that object (Milner et al., 2003). Consequently, a theory has been posited that assumes two separate pathways for the identification and for the localization of objects (Ungerleider et al., 1982). This theory has been initially supported by post-mortem inspection of the patients' brains, and more previously by monkey studies and human neuroimaging studies (Maunsell & Newsome, 1987; Shmuelof & Zohary, 2005). The common theme is that object identification and the impairment thereof is associated with the ventral temporal lobe of the brain, while the localization, for the purpose of manipulation, of objects is associated with the posterior parietal cortex. According to this theory, the ventral stream of object perception processes information such as shape, color, and texture for the purpose of identifying and categorizing an object. The

dorsal stream, in contrast, evaluates spatial information about the object. Hence, the two aspects identity and space are assumed to be encoded independently in separate cortical areas.

Recent fMRI studies have started to question this strict separation of information processing. High-level areas in the ventral stream appear to have similar characteristics as early visual areas. For example, FFA and LO in the left hemisphere show higher activation to faces and objets in the right, that is, contralateral side of the visual field (VF) than to faces and objects in the left, ipsilateral VF (Hemond, Kanwisher, & Op de Beeck, 2007) . Conversely, the same regions in the right hemisphere prefer stimuli in the left VF. Also, FFA as well as LO have been shown to prefer stimuli in the lower rather than the upper VF, while PPA is more activated for pictures in the upper than the lower VF (Schwarzlose, Swisher, Dang, & Kanwisher, 2008). Thus, there is ample evidence for certain VF biases, and therefore sensitivity to spatial location, in ventral stream areas. However, studies about location sensitivity have shown VF biases that comprise half of the VF (Hemond et al., 2007; Schwarzlose et al., 2008) or a quarter of the VF (Sayres & Grill-Spector, 2008) of the VF. It remains unknown to which detail, beyond half or quarter VFs, ventral stream areas can discriminate VF locations. Furthermore, it has not been investigated whether the VF biases of category-encoding areas are specific to the preferred object category or apply to all categories. Chapter 3 presents an fMRI study in which we systematically investigated which VF locations are represented in the ventral stream areas FFA and PPA. We show that a large proportion of these areas exhibit space sensitivity and that the areas as a whole exhibit the previously reported contralateral VF bias. Individual voxels[1] in FFA and PPA, however, are sensitive to stimulus locations in nearly the entire VF. Furthermore, we show that

[1] the smallest cortical partition that can be tested with fMRI

the representation of space is partially linked to the representation of category. We present a neural model that explains our findings.

2 Category selectivity in the ventral stream (experiment 1)

2.1 Introduction

Several decades of fMRI research have consistently located regions in the ventral stream that respond maximally to faces and houses, respectively (Bartels, Logothetis, & Moutoussis, 2008; Downing, Chan, Peelen, Dodds, & Kanwisher, 2006a; Grill-Spector & Malach, 2004; Op de Beeck, Haushofer, & Kanwisher, 2008). These areas have been termed the fusiform face area (FFA) and the parahippocampal place area (PPA) and have been shown to respond to face and house stimuli in various experimental settings and under various viewing conditions (Epstein, Harris, Stanley, & Kanwisher, 1999; Kanwisher et al., 1997). Researchers have consequently hypothesized that these regions selectively encode the category to which they respond the most (Aguirre, Zarahn, & D Esposito, 1998; Downing et al., 2006a; Epstein et al., 1999; Kanwisher et al., 1997; McCarthy, Puce, Gore, & Allison, 1997). (But see Gauthier & Tarr (Gauthier, Tarr, Andersen, Skudlarski, & Gore, 1999) for alternative interpretations especially of the function of FFA). The assumption is that category-selective regions are modules that are specialized for the recognition of a special category of objects and that do not operate on non-preferred object categories (Downing et al., 2006a; Kanwisher, 2000). Others have stressed the fact that the activation of ventral stream areas to their preferred category is maximal, but not exclusive, and that information about object categories is distributed throughout the ventral cortex (Haxby et al., 2001). Haxby and colleagues have proposed that ventral stream areas encode the low-level features of object categories. The maximal responses of different regions therefore reflect differences of low-level features in different object categories.

One way to test which of these theories reflect the true underlying neural computation is fMRI adaptation. fMRI adaptation (fMRI-A) relies on the assumption that a repeated stimulus leads to decreased activation in neural populations which are sensitive to that stimulus, but not in neural populations that are insensitive to that stimulus (Grill-Spector & Malach, 2001; Krekelberg, Boynton, & van Wezel, 2006). Two neural populations with different stimulus selectivity might be co-localized within the same voxel of an MR acquisition. This situation poses problems to conventional analysis techniques of the BOLD signal because they assess signal changes of the summed neural activity of a voxel. A typical fMRI voxel of 27mm³ comprises about 7 million neurons, which likely include neurons of various characteristics. For example, if a voxel contains neurons that encode the color green, as well as neurons that encode the color red, the averaged signal of both populations would be the same for green stimuli and for red stimuli. One might conclude, therefore, by looking at the average signal of a voxel to red and green stimuli, that the inspected voxel contains neurons which do not distinguish between, and thus are not sensitive to different colors. If, however, one repeatedly presents a green stimulus, then neural activation of the green-sensitive neurons decreases and consequently the average signal of the voxel decreases. The same decrease of activation would be observed for red stimuli. One can conclude that the voxel in question contains neurons that are selective for different colors, a conclusion which a conventional analysis would have failed to make. This aspect of fMRI-A makes it a suitable tool for studying neural selectivity for various stimulus characteristics. For example, studies using fMRI-A have exposed early visual areas that are selective for orientation, form, texture and color of stimuli (Cavina-Pratesi et al., 2010; Fang, Murray, Kersten, & He, 2005). fMRI-A has also been used to investigate sensitivity to viewpoint, translation, and size of high-

level ventral stream areas (Epstein, Graham, & Downing, 2003; Grill-Spector & Malach, 2001). Research on fMRI-A and stimulus selectivity is not restricted to low-level stimulus characteristics, but has also been used to get a different perspective on the controversy around category selectivity. The modular theory of category-selective regions would predict that adaptation is restricted to the preferred object category and does not occur for non-preferred categories. In contrast, if information of object category is distributed throughout the ventral cortex (Haxby et al., 2001) then ventral stream areas should show cross-category adaptation. The studies on fMRI-A and category selectivity have yielded contradicting findings. Some have found category-specific adaptation (Epstein et al., 1999; Pourtois, Schwartz, Spiridon, Martuzzi, & Vuilleumier, 2009) while others found evidence for cross-category adaptation (Avidan, Hasson, Hendler, Zohary, & Malach, 2002; Ewbank, Schluppeck, & Andrews, 2005; Mur, Ruff, Bodurka, Bandettini, & Kriegeskorte, 2010). There are at least two possible reasons for these mixed findings.

First, these studies have not controlled the low-level properties of stimuli. This fact might have confounded the results for the following reason. Some researchers claim that fMRI-A does not occur in the regions of interest themselves, but that it is "inherited" from early visual areas which adapt to low-level features of stimuli (Bartels et al., 2008; Krekelberg et al., 2006; Logothetis, 2008). V1 has been shown to be is sensitive to spatial frequency (SF) (Kaul, Bahrami, & Rees, 2009; Tootell, Silverman, & De Valois, 1981) and therefore should adapt to the repeated presentation of pictures with the same SF spectrum. Since visual information flows from V1 further to high-level object-selective areas, a reduction of signal strength in object-selective areas might be due to a reduced signal in V1. Thus, if one were to distinguish two theories for which

the presence or absence of adaptation is the critical factor lending support to one of the theories, one should exclude any potential adaptation effects originating from sources that are of no interest to the theories in question.

In this experiment we controlled for differences in the SF spectrum between face and house pictures by creating stimuli with an average SF spectrum. This was done by computing the SF spectrum of all the face and house pictures which we used and then reconstructing individual images by means of an inverse Fourier transformation using each image's phase spectrum and the average frequency spectrum of all stimuli. The resulting stimuli differed only in their phase spectra. Controlling the SF in this way should reduce any potential inheritance of adaptation from V1.

Second, the above-mentioned studies have employed two different experimental designs, block and event-related. In block design experiments stimuli are clustered in blocks of various lengths, usually between 5 and 20 seconds. Experimental conditions vary between blocks but are fixed within a block. Blocked experiments have the advantage of high statistical power, because a large number of experimental trials can be collected in a relatively short amount of time (Friston, Zarahn, Josephs, Henson, & Dale, 1999). The disadvantage is that participants can predict the majority of stimuli, since the first few stimuli of a block reveal its experimental condition and consequently the nature of the remaining stimuli (Pilgrim, Fadili, Fletcher, & Tyler, 2002). Thus, expectation might be a cognitive factor that confounds the experimental results. The problem of predictability can be avoided by using an event-related design. In event-related fMRI-A designs stimuli of one condition are presented individually or in pairs. In designs with individual stimulus presentations a scanning sequence consists of a multitude of randomly presented stimuli

that are either novel or repeated pictures. Other event-related designs group pairs of stimuli into "novel" and "repeated" conditions, where the first consists of two pictures which differ in the property of interest, while the latter consists of two identical pictures. Importantly, conditions can be varied on a trial-by-trial basis and can therefore change after each stimulus or pair of stimuli. Accordingly, the observer has no possibility of anticipating the nature of the following stimulus. The disadvantage of event-related designs is their relatively low statistical power compared to block designs. Events consist of only one or two stimuli and have to be separated by at least a few seconds, because the sluggish BOLD signal can otherwise not be unambiguously estimated during the statistical analysis. Consequently, in the same amount of time event-related designs yield fewer trials than block designs.

fMRI-A studies have employed both types of design, but few have compared adaptation effects between the two designs (but see Weiner et al. (Weiner, Sayres, Vinberg, & Grill-Spector, 2010) for a recently published comprehensive study on adaptation profiles in object-selective areas and the effect of experimental design). In this study we tested fMRI-A across object categories with both event-related and block designs.

To summarize, the purpose of this experiment was twofold. On the one hand we wanted to test two different views of the nature of high-level ventral stream areas by comparing fMRI adaptation across preferred and non-preferred object categories. On the other hand we employed and compared block and event-related experimental designs in order to assess any potential differences of adaptation effects between these two designs.

2.2 Methods

Participants

Thirteen healthy subjects (3 female, 12 right-handed) took part in the study (mean age 30.5 years; range 22 to 42 years). Participants had normal or corrected-to-normal vision and gave written informed consent prior to scanning. Participants were financially reimbursed for their participation. Scanning was performed at the CIMeC in Trento, Italy. Ethical approval was provided by the University of Trento, Italy.

Stimuli

The stimuli were generated on a PC at a frame rate of 60 Hz and projected onto a screen at the head end of the scanner bore. Participants viewed the screen via a mirror that is attached to the head cage of the coil. The distance between the eyes of the subjects and the screen was 134 cm. Custom software (ASF) (Schwarzbach, submitted) based on the Matlab Psychophysics Toolbox was used for stimulus presentation.

Images of 312 faces (downloaded from cswww.essex.ac.uk_faces94) and 312 houses (downloaded from the internet) were presented in the center of the screen (see **Figure 2.1** for example stimuli). The pictures were 252 by 252 pixels in size, which is equivalent to 3.45° visual angle. We equalized the pictures with respect to their average intensity and their spatial frequencies by computing the average SF spectrum of all face and house pictures. Each single picture was then reconstructed on base of the average frequency. Thus, all pictures had the same SFs and differed only with respect to their phase spectrum.

A red central fixation dot was present throughout each run. Since the stimuli were presented in the center of the screen, the fixation dot also marked the center of each picture. In order to minimize participants' eye movements we prepared the face pictures such that the center of each image was located at the onset of the nose and between the eyes of the depicted face. This was done because frontal faces are usually viewed at the level of the eyes and the nose (Bindemann, Scheepers, & Burton, 2009). The background color of the PC screen was dark gray.

Figure 2.1: Example stimuli for the adaptation experiment. Upper row: example face pictures; lower row: example house pictures. Pictures had the same spatial frequency, which was the average spatial frequency of all face and house pictures.

Experimental Design

Block Experiment

Participants viewed pictures of faces or houses while performing a color change detection task. Most of the pictures were grayscale images, but one picture per block (16 pictures per run) had a slight hint of red color. Participants' task was to press a mouse button upon detection of the red

hue. This type of task was chosen because it is unrelated to the experimental purpose, which was to determine whether a repetition of the same stimulus leads to reduced brain activation as compared to novel stimuli. There were two types of blocks, "same" and "different". "Same" blocks consisted of one picture that was repeatedly shown 12 times. "Different" blocks consisted of 12 different pictures. Each face or house exemplar was used only once during the entire experiment (including the event-related experiment), such that repetitions of pictures occurred only within a "same" block. Each block type was repeated 16 times and the order of "same" and "different" blocks was randomized. Blocks lasted 12 s and were separated by 10 s of fixation. Pictures were presented for 800 ms and were separated by 200 ms (**Figure 2.2 A**). A run started and ended with 16 s of a blank screen and lasted 374 s. Each participant performed two runs with face stimuli and two runs with house stimuli. Participants were instructed to fixate a central dot throughout the experiment.

Event-related Experiment

The event-related experiment employed the same task and conditions as the block experiment. Here, color changes occurred 6 times during a run. Stimuli were clustered in trials. A trial lasted 3400 ms and was characterized by two images shown in succession, each presented for 300 ms and separated by 400 ms of fixation (**Figure 2.2 B**). The second picture was followed by 2400ms fixation. As in the blocked experiment, there were two types of events. "Same" events consisted of the same picture presented twice, while "different" events consisted of 2 different pictures. Each event type was repeated 60 times. In addition, there were 60 fixation-only trials. The order of events was randomized. One event-related run lasted 338 s.

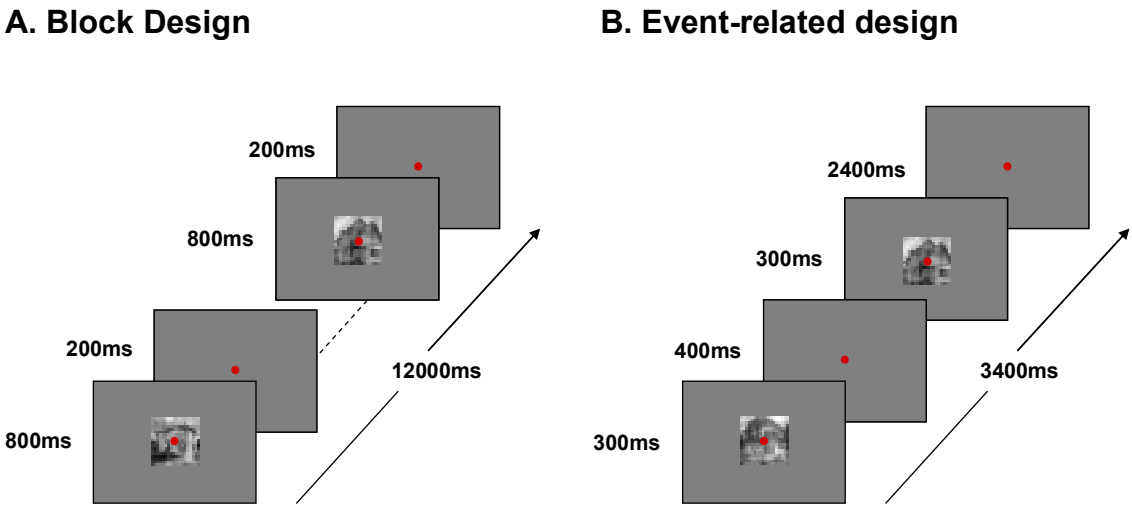

Figure 2.2: Experimental design of block and event-related experiments. A: An exemplary block of the "different" condition. One block consisted of 12 pictures which were presented for 800ms and which were separated by 200ms of fixation. A whole block lasted 1200ms. B: An exemplary trial in the event-related experiment. In a trial a pair of pictures was presented for 300ms, separated by 400ms fixation.

Localizer Experiment

The localizer experiment was intended to locate ventral stream areas that respond maximally to faces and houses, respectively. Participants saw pictures of faces, houses, objects and scrambled pictures and had to perform a one-back matching task. Twice during a block of stimuli an image was presented twice in a row and participants pressed a button when detecting this repetition. Blocks lasted 16 s and were separated by fixation blocks of 8 s. A block consisted of 20 images, that were shown for 300 ms were separated by 500 ms. A small black fixation cross was superimposed on the center of the pictures and remained visible between picture presentations. Each block type was repeated three times, adding up to 12 blocks and 396 s duration per run. A run started and ended with 8 s of a blank screen. Each participant conducted two runs of the localizer experiment.

The face images were provided by the Max-Planck Institute for Biological Cybernetics in Tübingen, Germany. The pictures were processed in the same way as for the main experiment. The average spatial frequency of all images was calculated and applied to each individual image.

Data Acquisition

Scanning was performed with a 4T Bruker MedSpec Biospin MR scanner and an 8-channel birdcage head coil. Functional images were acquired with a T2*-weighted gradient-recalled echo-planar imaging (EPI) sequence (TR = 2 s; TE = 33 ms; flip angle = 73°). Before each functional scan, we measured the point-spread function (PSF) of the scanning sequence in order to correct for high field distortions. We acquired 34 slices in ascending interleaved order approximately parallel to the calcarine sulcus (voxel resolution 3 x 3 x 3 mm; FoV = 192 x 192 mm; gap size = 0.45 mm). We also performed a high-resolution (1 x 1 x 1 mm^3) T1-weighted 3D MPRAGE anatomical sequence (sagittal slice orientation, image matrix = 256 x 224, FoV = 256 mm x 224 mm, 176 partitions with 1 mm thickness, GRAPPA acquisition with acceleration factor = 2, duration = 5.36 min, TR = 2700, TE = 4.18, TI = 1020 ms, 7° flip angle) for each participant.

Data Analysis

Data were analyzed with Brain Voyager QX version 1.10 (Brain Innovation, Maastricht, The Netherlands) and Matlab 7.3 (The MathWorks, Inc., USA). We discarded the first two volumes of each functional scan. Preprocessing of the functional data included 3D motion correction (trilinear interpolation), high-pass temporal filtering (GLM Fourier with 2 cycles), and slice scan time correction (cubic spline interpolation). Each functional scan was then co-registered to the

de-skulled anatomy in native space of each participant. The co-registered functional and anatomical were then transformed into a standardized (Talairach & Tournoux, 1988) space.

The functional data of the adaptation experiment were analyzed by fitting the regressors by means of the general linear model to the percent signal change (PSC) timecourse, confined to the regions of interest FFA and PPA. Experimental events (duration in the blocked experiment = 12 s; duration in the event-related experiment = 1 s) were convolved with a standard dual gamma hemodynamic response function (Delta 2.5, Tau 1.25). The predicted time courses of both the block and event-related experiments were then scaled to the maximum value 1, which allowed us to better compare the two designs. There were two regressors of interest (corresponding to the "same" and "different" conditions). The group data were analyzed with a fixed effects analysis with separate subject predictors.

The object localizer experiment analysis was not confined to any region, but was applied to all voxels in the data set. Blocks of stimulation were modeled as a box car function, which was convolved with a dual gamma hemodynamic response function (same parameters as in the adaptation experiment). Fixed-effects contrast analyses were performed to determine regions of interest (ROIs) in each individual participant. FFA was determined by contrasting faces with houses, tools, and scrambled pictures. Similarly, PPA was determined with the contrast houses versus faces, tools and scrambled pictures. The resulting parameter maps were thresholded at a false discovery rate (FDR) (Genovese, Lazar, & Nichols, 2002) of $q < 0.05$ and were used to outline the two ROIs.

2.3 Results

The goal of this experiment was to test whether the ventral stream regions FFA and PPA encode selectively their respective preferred stimulus categories. We employed the technique of fMRI-A, which is commonly used to detect brain regions that have a decreased BOLD signal in trials where the same stimulus is repeated as compared to trials where different stimuli are shown. Such a decrease in activation is referred to as fMRI-A. It is assumed that only those regions show fMRI-A which encode the stimulus characteristic that is varied between the two types of blocks. We have used fMRI-A to test whether the object-selective regions FFA and PPA encode selectively their preferred object category, that is, faces or houses, or whether they also encode aspects of their non-preferred categories. We therefore varied the stimulus category (faces or houses) and probed to which conditions these brain regions would adapt. If FFA and PPA encode selectively the high-level aspects of their preferred stimuli, then they should have a decreased activation to the repeated presentation of the preferred stimuli, but not to the repeated presentation of the non-preferred stimulus category.

Because there have been contradicting results of adaptation effects in block and event-related designs, we tested cross-category adaptation with both block and event-related designs. In the following sections I will first present the results of the block design experiment, followed by the results of the event-related design, and finally I will report calculations that compare the two designs.

Localization of FFA and PPA

We defined FFA and PPA in each participant by overlaying the contrast parameter maps on the anatomical data and outlining all continuously activated voxels that lay within the fusiform gyrus and the parahippocampal gyrus, respectively. FFA was localized in the right hemisphere of all 13 participants, and in the left hemisphere of 12. PPA was located in both hemispheres of all participants. **Table 2.1** lists the mean Talairach coordinates for both regions of interest (ROIs) in the left and right hemispheres. For the following analyses we averaged the left and right hemispheres to form a single face area and a single house area.

Table 2.1: Mean Talairach coordinates for FFA and PPA, derived from all 13 participants in the localizer experiment.

	Left			Right		
	X	Y	Z	X	Y	Z
FFA	-27.15 ± 22.01	-49.02 ± 9.83	-15.57 ± 4.43	35.91 ± 2.35	-48.95 ± 5.25	-15.42 ± 2.67
PPA	-26.03 ± 1.93	-45.23 ± 4.09	-11.00 ± 2.14	23.94 ± 3.07	-43.94 ± 4.15	-10.85 ± 2.35

Values represent the mean ± std in mm.

Adaptation profiles in the block design

In the block design experiment we presented participants with blocks of stimuli that were either repetitions of the same exemplar ("same" condition) or 12 different exemplars of a category ("different" condition). **Figure 2.3** depicts the estimated activation strengths (beta weights) of FFA and PPA for the categories faces and houses and for the two experimental conditions "different" and "same". FFA (left panel) has a stronger activation for faces (blue line) than for houses (green line), whereas PPA (right panel) has a stronger activation for houses than for faces. To test for adaptation effects, i.e. signal decrease for repetitions with respect to non-

repetitions, and for categorical preferences for ROIs we submitted the fitted beta weights to a repeated measures ANOVA with ROI (FFA, PPA), condition (same, different) and category (preferred, non-preferred) as within-subject factors. Both ROIs showed stronger activation for their respective preferred category (main effect category: $F(1,12) = 49.178$, $p < 0.001$) with no significant interaction of ROI and category ($F(1,12) = 3.254$, $p = 0.096$). Note that category was coded as preferred/ non-preferred. Both ROIs exhibited adaptation as their respective signals decreased in the "same" compared to the "different" condition (main effect condition: $F(1,12) = 125.71$, $p < 0.001$).

Of main interest for this study was, however, whether the adaptation effect is selective to the preferred stimulus category. Such a selective adaptation would be suggested by an interaction of category and condition. This interaction was indeed significant ($F(1,12) = 62.342$, $p < 0.001$). The interaction can be seen in **Figure 2.3** by the fact that the line between the "different" and "same" conditions drops more steeply for the preferred category (faces for FFA and houses for PPA) than for the non-preferred category. In order to validate that the interaction is in fact due to reduced beta weights in the "same" condition we computed an adaptation index (AI) for the preferred and non-preferred categories and compared these with paired-samples t-tests. For computing the AI we subtracted the beta weight of the "same" condition from the beta weight of the "different" condition, separately for each participant. Positive values of this index indicate adaptation, and the higher the value the stronger the adaptation effect. No effect of condition would be reflected by a value of zero. **Figure 2.4** shows the group means of AIs (see **Table 2.2** for an overview of all beta weights and AIs). The AIs of both FFA (left panel) and PPA (right panel) are higher for the preferred than for the non-preferred categories. This effect was

confirmed with a paired-samples t-test comparing the AIs of preferred and non-preferred categories (in FFA: $t_{12} = 8.524$, $p < 0.001$; in PPA: $t_{12} = 3.68$, $p = 0.003$; all t-tests two-tailed).

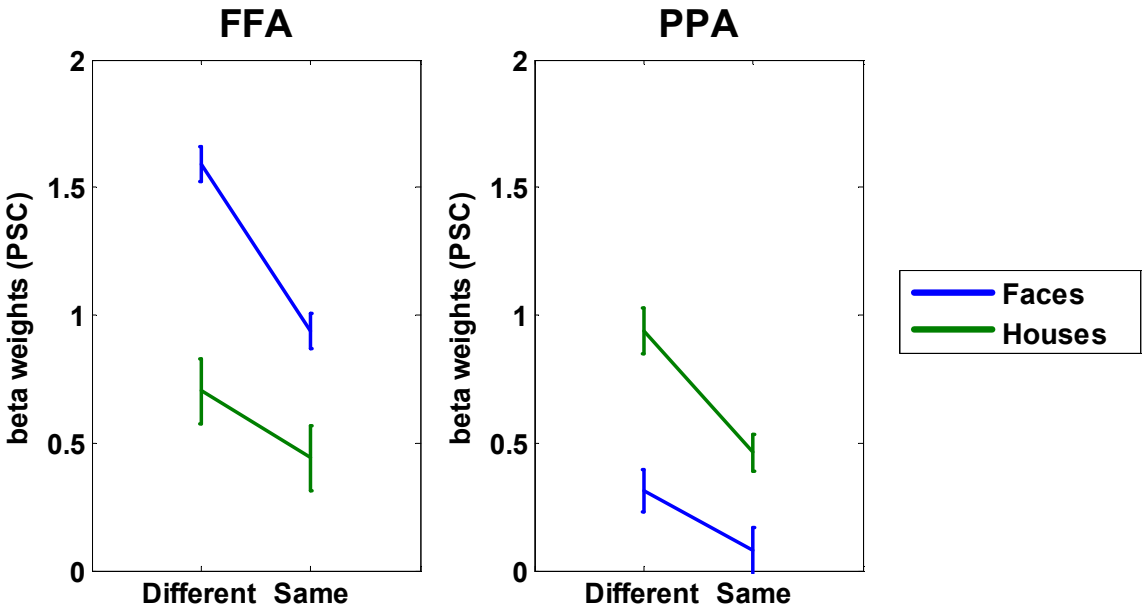

Figure 2.3: Activation strength in FFA and PPA in the block design experiment. Shown are the mean beta weights (n = 13) for the stimulus categories faces (blue lines) and houses (green lines) and for the two conditions "different" and "same" (x-axis). In the condition "same" participants saw blocks with 15 repetitions of the same exemplar of a category (faces or houses), in the condition "different" they saw 15 different exemplars of a category. Error bars are the standard error of the group mean.

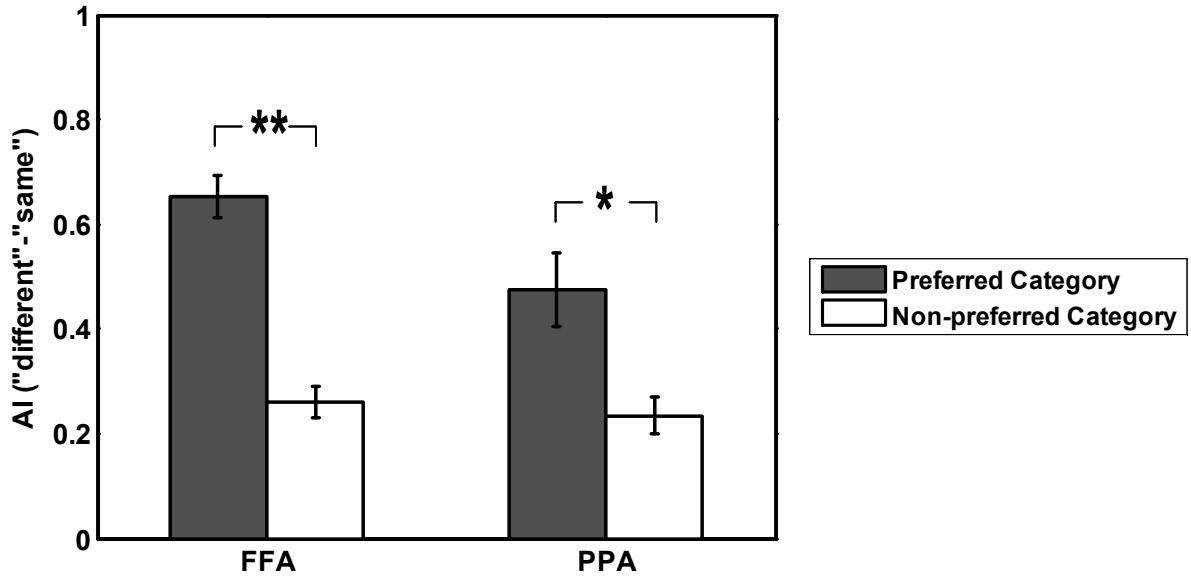

Figure 2.4: Adaptation indices of FFA and PPA for the preferred and the non-preferred categories (block design). Adaptation is significantly higher for the preferred than for the non-preferred categories. The adaptation index (AI) is the difference between the condition "different" and the condition "same". Dark grey bars are the group mean (n = 13) of AIs for the preferred category (faces for FFA, houses for PPA); white bars are the group mean of AIs for the non-preferred categories (houses for FFA, faces for PPA). Error bars are the standard error of the group mean. ** = significant at p<0.001; * = significant at p<0.01.

Adaptation profiles in the event-related design

The experimental trials in the event-related design consisted of pairs of stimuli that were either one object exemplar repeated once or two different exemplars. We used exemplars of faces or houses and tested which of our two ROIs would show adaptation to the two categories. The activation strengths of FFA and PPA to the different conditions can be seen in **Figure 2.5**. As in the block design, the activation in FFA is higher for faces than for houses, while PPA responds stronger to houses than to faces. Both ROIs show a decreased activation in the "same" condition as compared to the "different" condition. This decrease in activation is similar for faces and for houses, as can be seen by the fact that the two lines are nearly parallel. We computed a repeated-measures ANOVA with the factors ROI (FFA, PPA), category (preferred, non-preferred) and

condition (same, different) to assess the statistical significance of the observed effects. As in the block design, both ROIs showed higher activation for their respective preferred categories (main effect category: $F(1,12) = 133.66$, $p < 0.001$), but in the event-related design this effect was stronger in FFA than in PPA (interaction of ROI and category: $F(1,12) = 15.687$, $p = 0.002$), as can be seen in **Figure 2.5** by the fact that the blue and green lines, representing activation to faces and houses, are further apart in FFA than in PPA. Furthermore, there was a significant main effect of condition ($F(1,12) = 10.239$, $p = 0.008$), which represents a significant adaptation to the repeated presentation of stimuli. In the event-related design there was also evidence for the hypothesis that regions adapt stronger when their preferred stimulus as opposed to their non-preferred stimulus is shown (significant interaction of category and condition $F(1,12) = 5.58$, $p = 0.036$).

We computed adaptation indices for the preferred and for the non-preferred categories in the same way as we did for the block design. In **Figure 2.6** we plot the group mean of individual AIs. In line with the block design experiment, the AIs are higher for the preferred than for the non-preferred categories. However, here the difference of mean AIs between preferred and non-preferred categories is not significant (FFA: $t_{12} = 1.929$, $p = 0.078$; PPA: $t_{12} = 0.55$, $p = 0.593$; paired-samples t-tests comparing the AIs between preferred and non-preferred categories).

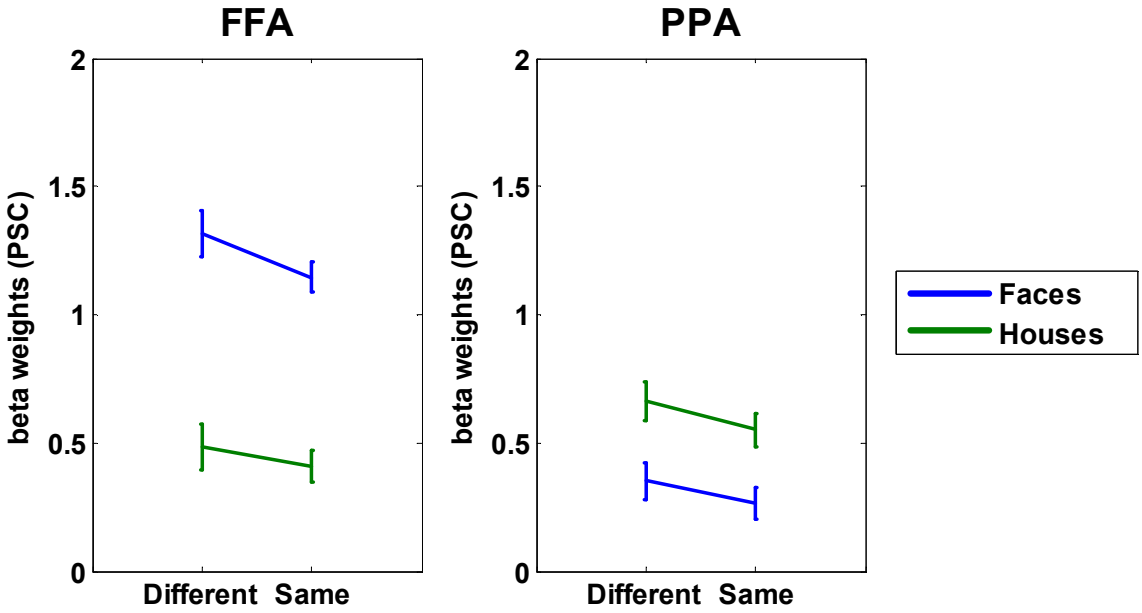

Figure 2.5: Activation strength in FFA and PPA in the event-related design experiment. Shown are the mean beta weights (n = 13) for the stimulus categories faces (blue lines) and houses (green lines) and for the two conditions "different" and "same" (x-axis). In the condition "same" participants saw a pair of identical pictures, in the condition "different" they saw a pair of two different exemplars of a category (faces or houses). Error bars are the standard error of the group mean.

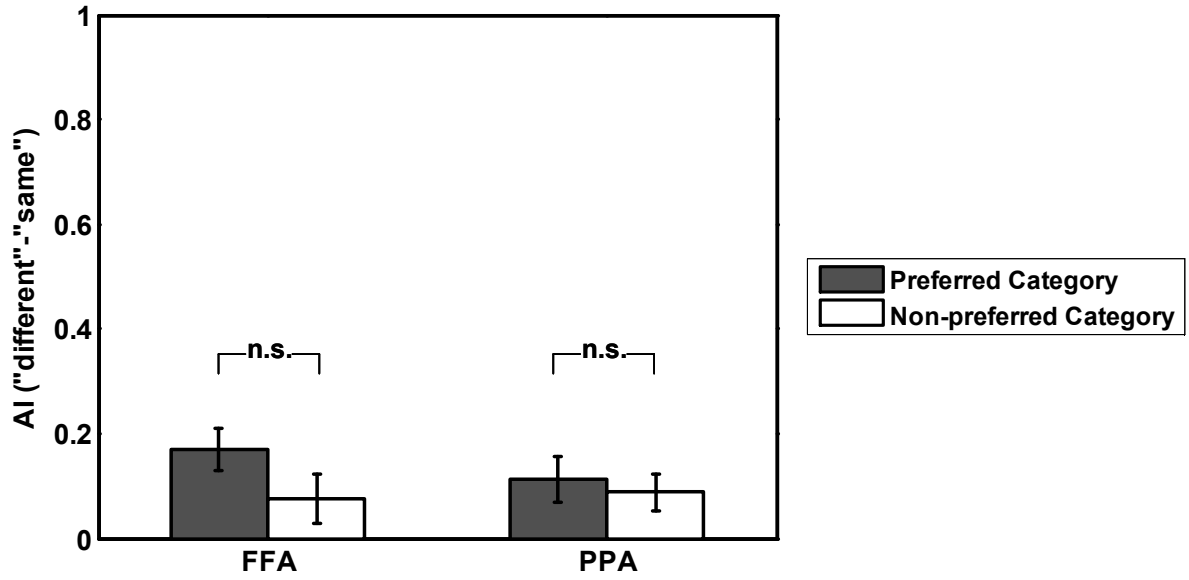

Figure 2.6: Adaptation indices of FFA and PPA for the preferred and the non-preferred categories (event-related design). There is no significant difference of adaptation between the preferred and the non-preferred categories. The adaptation index (AI) is the difference between the condition "different" and the condition "same". Dark grey bars are the group mean (n = 13) of AIs for the preferred category (faces for FFA, houses for PPA); white bars are the group mean of AIs for the non-preferred categories (houses for FFA, faces for PPA). Error bars are the standard error of the group mean.

Table 2.2: Mean beta weights and adaptation indices in the block and event-related designs (n = 13).

			mean Beta (std)		mean AI (std)
			"same"	"different"	
Block Design	FFA	Preferred (faces)	0.94 (0.25)	1.59 (0.25)	0.65 (0.04)
		Nonpreferred (houses)	0.44 (0.46)	0.70 (0.46)	0.26 (0.03)
	PPA	Preferred (houses)	0.46 (0.27)	0.94 (0.32)	0.48 (0.07)
		Nonpreferred (faces)	0.08 (0.31)	0.31 (0.31)	0.23 (0.04)
Event-related Design	FFA	Preferred (faces)	1.15 (0.22)	1.32 (0.32)	0.17 (0.04)
		Nonpreferred (houses)	0.41 (0.23)	0.49 (0.32)	0.08 (0.05)
	PPA	Preferred (houses)	0.55 (0.24)	0.67 (0.27)	0.11 (0.04)
		Nonpreferred (faces)	0.26 (0.22)	0.35 (0.27)	0.09 (0.03)

Means and standard deviations of beta weights and adaptation indices (AIs) of 13 participants. Beta weights reflect percent signal change; the AI is the difference between beta weights of the “different” and “same” conditions.

Comparison of block and event-related designs

In the previous two paragraphs it appears that the block and event-related designs yielded many similar effects and a few differences. In both designs we found that the BOLD signal was higher for preferred than for non-preferred categories, and higher when pictures were novel than when they were repeated, indicating adaptation to the stimulus. Furthermore, in both designs this adaptation was higher when the stimuli belonged to the preferred category rather than the non-preferred category. In contrast, in the event-related design, but not in the block design, FFA showed higher category preference than PPA. Also, when we investigated the AIs in the two ROIs we found that they were significantly higher for preferred than for non-preferred categories in the block design while they did not differ in the event-related design. In order to test the general tendencies in the data set, and to see whether there were substantial differences between

the two designs, we submitted the whole data set to a repeated-measures ANOVA with the factors design (block, event-related), ROIs (FFA, PPA), category (preferred, non-preferred) and condition (same, different) with the estimated BOLD amplitude being the dependent variable.

There was no difference in BOLD amplitude between designs (main effect design: $F(1,12) = 0.241$, $p = 0.632$). The activation to preferred categories was higher than that to non-preferred categories (main effect category: $F(1,12) = 80.34$, $p < 0.001$), and this category preference did not differ between the two designs (interaction of design and category: $F(1,12) = 1.14$, $p = 0.306$). The overall model also yielded a highly significant adaptation effect (main effect condition: $F(1,12) = 175.85$, $p < 0.001$), but the amount of adaptation differed between the two designs (interaction of design and condition: $F(1,12) = 24.797$, $p < 0.001$). This interaction reflects the fact that the adaptation effect was stronger in the block design than in the event-related design, as indicated by the relatively higher AIs in the block design (for example, the mean group AI of FFA for faces was 0.65 (std 0.04) in the block design and 0.17 (0.04) in the event-related design; see **Table 2.2**). Furthermore, adaptation was stronger for preferred than for non-preferred categories (interaction of category and condition: $F(1,12) = 39.079$, $p < 0.001$), but this enhanced adaptation for preferred categories was more pronounced in the block design (three-way interaction of design, category and condition: $F(1,12) = 79.711$, $p < 0.001$).

As mentioned above, the event-related design indicated that the two ROIs differed with respect to the amount of their category preference. Also in the overall model we found stronger category preference in FFA than in PPA (interaction of ROI and category: $F(1,12) = 13.302$, $p = 0.003$; remember that category was coded as “preferred” and “non-preferred”). In fact, even though this effect was not significant in the block design, the beta weights for faces and houses in **Figure 2.3** are further apart in FFA than in PPA, indicating that also in the block design there was a

tendency that FFA is more selective than PPA. The other difference between the designs was that in the block design the AIs were higher for preferred than for non-preferred categories while this effect was absent in the event-related design. A repeated measures ANOVA with AI as the dependent variable and with the factors design (block, event-related), ROIs (FFA, PPA) and category (preferred, non-preferred) confirmed the effect in the block design (main effect of category: $F(1,12) = 39.181$, $p < 0.001$).

So far we have investigated adaptation effects in FFA and PPA to preferred and non-preferred categories by comparing the amount of adaptation between categories. However, if we want to detect adaptation that is entirely specific to the preferred category, as would be predicted by a modular view of category encoding, we have to look for the absence of adaptation for non-preferred categories. We therefore inspected the effect of adaptation more closely by computing paired samples t-tests on the beta weights for the "same" and "different" conditions, separately for each category and ROI. In the block design, the difference between the two conditions was highly significant for both preferred (FFA: $t_{12} = 15.796$, $p < 0.001$; PPA: $t_{12} = 6.399$, $p < 0.001$) and non-preferred categories (FFA: $t_{12} = 8.264$, $p < 0.001$; PPA: $t_{12} = 6.347$, $p < 0.001$). Similarly, in the event-related design PPA showed significant adaptation for both preferred ($t_{12} = 2.447$, $p = 0.031$) and non-preferred ($t_{12} = 2.467$, $p = 0.03$) categories. Interestingly, however, for FFA this difference was significant only for the preferred category ($t_{12} = 3.63$, $p = 0.003$), but not for the non-preferred categories ($t_{12} = 1.89$, $p = 0.083$).

Adaptation profiles in V1

In four participants we also localized the early visual area V1. We analyzed V1 activation in the block and the event-related adaptation experiments in order to test whether V1 shows adaptation

to the repeated presentation of stimuli and might therefore be the actual source of adaptation effects in FFA and PPA. The mean group activation of FFA, PPA and V1 for the different conditions is plotted for both the block and event-related design in Error! Reference source not found. (and see Error! Reference source not found. for an overview of all mean beta weights and AIs of the four participants included in this analysis). Adaptation effects are indicated by a drop of activation from the "different" condition to the "same" condition. Such a drop can be seen in FFA and PPA in both designs, but in V1 it seems to be nearly absent in the block design. To quantify these effects we computed an ANOVA with the factors design (block, event-related), ROI (FFA, PPA, and V1), category (faces, houses) and condition (same, different) with the estimated BOLD amplitude as dependent variable. The results suggest that adaptation effects differ in the three ROIs, as indicated by an interaction of ROI and condition ($F(2,6) = 13.396$, $p = 0.006$; sphericity assumed). This effect was different in the two designs (interaction of design, ROI and condition; $F(2,6) = 21.1$, $p = 0.002$; sphericity assumed). We investigated further in which way the two designs affected the interaction of ROI and condition by computing ANOVAs separately for each design. In the block design different ROIs showed different BOLD signal amplitudes (interaction of ROI and condition: $F(2,6) = 54.65$; $p < 0.001$), while this did not occur in the event-related design (interaction of ROI and condition: $F(2,6) = 0.254$, $p = 0.783$). The above mentioned tests assess the differences between all three ROIs, rather than directly comparing object-selective ROIs with V1. Therefore, we also tested adaptation effects separately for each ROI and in each design. To this means we computed six ANOVAs with the factors category and condition for the dependent variable estimated BOLD signal amplitude. In the block design, both FFA and PPA showed significant adaptation effects (FFA: $F(1,3) = 59.13$, $p = 0.005$; PPA: $F(1,3) = 21.56$, $p = 0.019$) while V1 did not ($F(1,3) = 8.35$, $p = 0.063$). In

contrast, the event-related design yielded significant adaptation effects in PPA ($F(1,3) = 14.69$, $p = 0.031$) but neither in FFA ($F(1,3) = 2.02$, $p = 0.251$) nor in V1 ($F(1,3) = 3.66$, $p = 0.152$).

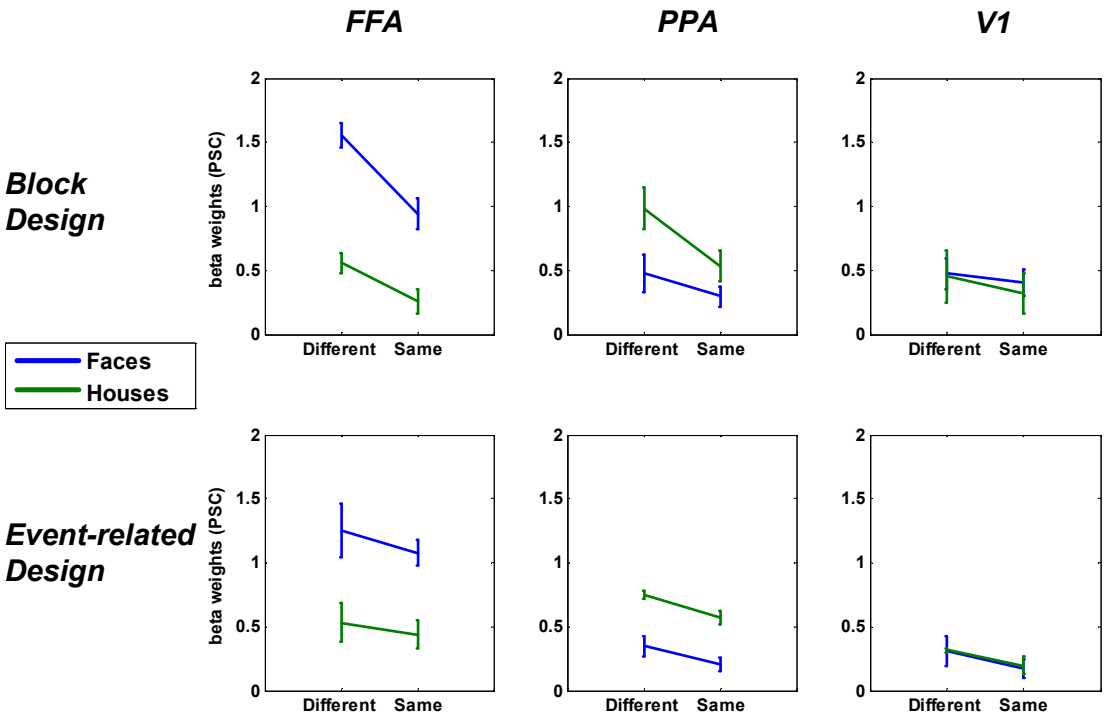

Figure 2.7: Adaptation effects in FFA, PPA and V1 (n = 4). Mean beta weights of four participants in the block design experiment (upper row) and the event-related design (lower row) for three areas FFA, PPA and V1 (columns 1 to 3).

Table 2.3: Mean beta weights and adaptation indices in the block and event-related designs (n = 4).

			mean Beta (std)		mean AI (std)
			"same"	"different"	
Block Design	FFA	Faces	0.94 (0.25)	1.55 (0.19)	0.61 (0.05)
		Houses	0.26 (0.19)	0.56 (0.16)	0.30 (0.07)
	PPA	Faces	0.30 (0.16)	0.48 (0.29)	0.18 (0.07)
		Houses	0.53 (0.24)	0.98 (0.33)	0.45 (0.09)
	V1	Faces	0.40 (0.22)	0.47 (0.24)	0.07 (0.04)
		Houses	0.32 (0.32)	0.45 (0.41)	0.14 (0.05)
Event-related Design	FFA	Faces	1.08 (0.20)	1.25 (0.42)	0.17 (0.11)
		Houses	0.44 (0.22)	0.53 (0.30)	0.09 (0.07)
	PPA	Faces	0.21 (0.10)	0.35 (0.15)	0.14 (0.04)
		Houses	0.57 (0.11)	0.75 (0.06)	0.18 (0.05)
	V1	Faces	0.17 (0.14)	0.31 (0.22)	0.13 (0.08)
		Houses	0.20 (0.14)	0.32 (0.04)	0.12 (0.06)

2.4 Discussion

Evidence for cross-category adaptation

In the block as well as the event-related design cross-category adaptation was indicated by the fact that adaptation was present for both the preferred and the non-preferred categories. This is in line with previously reported cross-adaptation effects. Avidan and colleagues (Avidan et al., 2002) located face- and house-selective regions in the posterior fusiform gyrus and the collateral sulcus, respectively, and tested adaptation in these regions to the presentation of faces, houses and words. Both regions adapted significantly to the repeated presentation of stimuli, and this effect was the same for the three types of stimuli. Cross-category adaptation was also found by Ewbank et al. (Ewbank et al., 2005), who reported adaptation effects in FFA and PPA for inanimate object stimuli. Furthermore, a recent study by Weiner et al. (Weiner et al., 2010) yielded significant adaptation effects in face- and house-selective regions to faces, limbs, flowers, cars, guitars, and houses. Thus, our results, in line with other studies, suggest that ventral stream regions encode stimulus properties not only of preferred categories but also of non-preferred categories.

However, there are also indications that adaptation is stronger for the preferred than for the non-preferred categories. In our experiment the effect of adaptation was significantly stronger for preferred than for non-preferred categories. A recently published study by Weiner and colleagues (Weiner et al., 2010) compared, similar to our study, adaptation profiles across categories between block and event-related designs. In line with our results, they found an increased adaptation effect for preferred categories compared to non-preferred categories. This effect was

found in face- and house-selective areas in a block design experiment, as well as in a face-selective area in the event-related experiment. In the event-related experiment, however, the house-selective area did not show increased adaptation to houses, but instead showed less adaptation to houses than to other, non-preferred categories. In our event-related study, in contrast, the overall ANOVA yielded a significant interaction of category preference and adaptation effect, and this effect was not significantly different between FFA and PPA, as there was no interaction between category, condition and ROI. Yet, when we looked at the two ROIs in isolation, we found that a) the differences between preferred and non-preferred categories were not significant, and b) the difference was nevertheless larger in FFA than in PPA (mean AIs for preferred and non-preferred categories in FFA: 0.17 (std 0.04) and 0.08 (0.05), $p = 0.078$; and in PPA: 0.11 (0.04) and 0.09 (0.03), $p = 0.593$). Thus, we saw a similar trend in our data as Weiner and colleagues. But our results suggest that the absence of category-preference in the adaptation effect in PPA is related to low power of the event-related design to detect adaptation effects in single ROIs, since the effect across ROIs was significant. Also, if we compare the AIs between the block and the event-related designs, we see that the event-related design led to less adaptation than the block design (**Figure 2.4** and **Figure 2.6**). Accordingly, it appears that the differences between the two designs are due to lower detection power in the event-related design rather than to qualitative differences in the category-encoding characteristics of FFA and PPA. The findings mentioned so far indicate that adaptation is either equal for preferred and non-preferred categories, or that it is stronger for the preferred category. Both effects speak against a strongly modular theory of object representation, because they demonstrate sensitivity to non-preferred categories. But, there is also some evidence for category-specific sensitivity.

Little evidence for category-specific adaptation

We found some support for the notion of category-specific adaptation when directly comparing the activation to the "different" and "same" conditions of the individual ROIs. The event-related design yielded an adaptation effect in FFA only for faces and an absence of adaptation for houses. Similarly, even though the study by Ewbank et al. (Ewbank et al., 2005) revealed FFA adaptation to inanimate objects, FFA nevertheless showed no adaptation to house stimuli. In the same line, face-specific adaptation in FFA and house-specific adaptation have been reported by Pourtois et al. (Pourtois et al., 2009) and Epstein et al. (Epstein et al., 1999), respectively. Thus, the existence of category-specific adaptation cannot be ruled out completely. Interestingly, our experiment also indicated that the response of FFA, averaged over "same" and "different" conditions, is more selective for faces than that of PPA is for houses. Accordingly, it is not surprising that FFA also exhibits more selectivity in its adaptation profile than PPA. But how trustworthy is the absence of an adaptation effect for the non-preferred category that we saw in the event-related design in FFA? After all, the block design yielded adaptation effects for both categories, and so did the full event-related model (that is, when performing an ANOVA with FFA and PPA). If we look at the height of the bars in **Figure 2.4** and **Figure 2.6** (and see **Table 2.2** for the exact values) we get an indication that detection power for an adaptation effect was lower in the event-related as compared with the block design. Consequently, the category-specific adaptation effect in FFA appears to be the result of low power in the event-related design compared with block design.

It is unlikely that our results were caused by adaptation effects that actually occurred in V1 and were then fed forward to FFA and PPA. The analyses of V1 activation in the block design gave

no indication that V1 showed adaptation to either faces or the houses, while the object-selective areas FFA and PPA did show such an adaptation. For the event-related design the results were less assuring, because even though V1 did not show a significant adaptation effect, neither did FFA. However, these results have to be regarded with caution, because they are based on only four participants and might therefore not be generalizable.

In sum, our two experiments yielded highly significant effects of adaptation for the two tested categories, and these effects were stronger for the preferred as compared with the non-preferred categories. Such a picture fits well into the theory of a distributed representation of category information where clusters of similar object characteristics form areas that respond maximally, but not exclusively to one category.

3 Space sensitivity in the ventral stream (experiment 2)

3.1 Introduction

The predominant view of visual object perception assumes a separation of information processing into two pathways (Ungerleider et al., 1982). It is postulated that the dorsal stream evaluates spatial aspects of the visual information with the purpose of interacting with an object. This processing stream starts in V1, the first cortical area to receive visual input, and extends into the parietal lobe. The ventral stream, on the other hand, processes information about the identity of the visual stimulus. The starting point of this pathway is also V1, and it then reaches into the ventral temporal lobes. The final processing steps of the ventral stream takes place in the high-level visual areas LO, EBA, FFA, and PPA, which have been shown to correlate highly with the identification and categorization of objects, body parts, faces, and houses, respectively (Yovel & Kanwisher, 2005). Visual information reaches V1 in a retinotopically preserved manner, that is, two adjacent points on the retina will be encoded next to each other on the cortical surface of V1. Further along the ventral stream, however, the representation of the object becomes more abstract, until it is completely size- , viewpoint- and translation-invariant in the high-level visual areas (Ungerleider et al., 1982). Recent studies have questioned the absence of location information in the object-encoding areas. Hemond et al. (Hemond et al., 2007) found a contralateral visual field (VF) bias in FFA and LO, which formerly has been known only for early visual areas. Schwarzlose and colleagues (Schwarzlose et al., 2008) found that FFA had higher activation when stimuli were presented in the lower VF than when they were presented in

the upper VF. In contrast, PPA preferred the upper VF over the lower VF. A more complex assessment of VF preferences has been done by Sayres and Grill-Spector (Sayres & Grill-Spector, 2008). They presented object pictures at six different locations of the VF and measured activation strength in LO. They found that LO had a bias for the lower contralateral VF and that position effects were stronger than category effects.

These studies have applied an analysis that is based on the mean BOLD signal of an area. Studies on the representation of space in early visual areas, however, usually make use of a phase-encoded design and analysis. Such phase-encoded analysis evaluates each individual voxel within a ROI according to how well the timecourse of the response pattern correlates with the timecourse over which stimulus location is continuously varied. In early visual areas this has revealed full retinotopic maps of the contralateral VF (Engel et al., 1994; Sereno et al., 1995). The established retinotopic areas V1, V2 and V3 have been defined with fMRI by outlining the borders of one VF map. More recently, many other visual areas have been defined according to their VF map: the dorsal maps V3A, V3B, V6, and IPS0-4, the lateral maps LO-1, LO-2, and hMT, and finally the ventral maps hV4, VO-1, VO-2 (Wandell, Dumoulin, & Brewer, 2007). In 2009, yet another two areas have been found (Arcaro, McMains, Singer, & Kastner, 2009). PHC-1 and PHC-2 are located at the ventral stream, anterior of the ventral occipital retinotopic areas VO-1 and VO-2. Interestingly, these areas not only had a full retinotopic map, but they also responded preferentially to pictures of houses as compared to other object categories. Such selective activation for one object category is the defining characteristic of high-level visual areas, which in turn have always been regarded as being insensitive to space. Also Sayres and Grill-Spector (Sayres & Grill-Spector, 2008) used a phase-encoded retinotopic mapping experiment with checkerboard stimuli to investigate space sensitivity in LO. LO indeed showed

position modulation and a bias for the lower contralateral VF. So far no retinotopic mapping experiment has demonstrated VF maps in the object-selective areas FFA and PPA.

In summary, several studies have found indications for space-sensitivity in object-selective ventral stream areas, and thus undermine the established view of an abstract encoding of object identity. These studies have not, however, investigated in which detail object-selective areas encode space, as they used at most six stimulus locations. Furthermore, most of these studies have analyzed the mean signal of a region of interest (ROI). An exception is Arcaro et al. (Arcaro et al., 2009), who applied a voxel-based analysis and stimulated the entire VF. However, these authors were interested in detecting areas with similar retinotopic properties as the early visual areas. Accordingly, they used regular retinotopic mapping stimuli, which are low-level checkerboard patterns and are an optimal stimulation for early visual areas. However, checkerboard patterns are non-optimal stimuli for high-level visual areas, which respond mainly to objects and maximally to their preferred object categories. Accordingly, it is not surprising that previous studies have not found visual field maps in object-selective areas.

In this study we wanted to investigate the extent of space sensitivity in the face-selective fusiform face area (FFA) and the house-selective parahippocampal place area (PPA). For this purpose we combined a phase-encoded retinotopic mapping design with the presentation of face and house pictures, the preferred stimuli of FFA and PPA. We hypothesized that if FFA and PPA have a similar representation of space as early visual areas, then this representation might be detected only with pictures of the preferred categories, that is, of faces and houses. In addition, we used pictures of tools as well as Fourier-scrambled pictures. The former served as a comparison of the representation of space between the preferred category and a non-preferred category. Scrambled pictures were used in order to test whether a representation of space also

exists for low-level stimuli. To our knowledge, this is the first study that used a retinotopic mapping procedure with object stimuli and in combination with an ROI-based analysis.

3.2 Methods

Eight healthy participants (3 male, 7 right-handed) took part in the study (mean age 32 years; range 28 to 42 years). Participants had normal or corrected-to-normal vision and gave written informed consent prior to scanning. Participants received 15€ per hour for their participation. Scanning was performed at the CIMeC in Trento, Italy. Ethical approval was given by the University of Trento, Italy.

Participants performed three different experiments. For the localization of high-level object-selective areas and the early visual area V1 they performed an object category localizer experiment and a standard retinotopic mapping experiment, respectively. For the main experiment, in which we combined a retinotopic mapping design with the presentation of object stimuli, we acquired eight polar angle mapping runs with objects (faces, houses, tools, scrambled objects; rotation clockwise and counter clockwise) and eight eccentricity mapping runs (faces, houses, tools, scrambled objects; expanding and contracting). Scanning was performed in several sessions (3 to 4) to complete the whole set of experiments. The stimuli were generated on a PC at a frame rate of 60 Hz and projected onto a screen at the head opening of the scanner bore. Participants viewed the screen via a mirror that was mounted on top of to the head coil. The distance between the eyes of the participants and the screen was approximately 134 cm. We used ASF (ASF) (Schwarzbach, submitted), an experimental framework based on the Matlab Psychophysics Toolbox (Brainard, 1997; Pelli, 1997) for stimulus presentation.

Localizer experiment for object-selective areas

As we were interested in space sensitivity of ventral temporal lobe areas, we refined our analyses to the face- and house-selective areas FFA and PPA. These areas were defined in a separate localizer experiment in which pictures of faces, houses, tools, and Fourier-scrambled objects were presented in the center of the screen. Fourier scrambling was performed by submitting all grayscale images to a fast Fourier transform, yielding individual frequency and phase spectra. We averaged all frequency spectra and recreated a scrambled version of each image by inverse Fourier transform (IFFT) of the average frequency spectrum and the permuted phase spectrum of the given image. After all images had been reconstructed by means of IFFT we normalized them to the same average intensity. We chose to use a fixed central stimulus location because we wanted our definition of the regions of interest (ROIs) to be comparable with the way these areas are generally defined in the literature (Downing, Chan, Peelen, Dodds, & Kanwisher, 2006b; Kanwisher et al., 1997). Furthermore, we did not want the definition of ROIs to be biased by any spatial information.

Participants performed a one-back matching task. Twice during a block the same image was immediately repeated. Participants were asked to press a button when detecting this repetition. Blocks of different stimulus classes were shown in random order. Each stimulation block lasted 16 s and was separated by the next block with an 8 second fixation period. There were 20 images in a block, each presented for 300 ms and separated by the next image with an ISI of 500ms. A small black fixation cross was superimposed on the center of the pictures and remained visible between picture presentations. Each block type was repeated three times, adding up to 12 blocks and 396 s duration per run. Participants performed two runs of the localizer experiment.

The face database was provided by the Max-Planck Institute for Biological Cybernetics in Tübingen, Germany. The house and tool pictures have been used and described in previous studies (Mahon, Anzelotti, Schwarzbach, Zampini, & Caramazza, 2009; Serences, Schwarzbach, Courtney, Golay, & Yantis, 2004).

Standard retinotopic mapping

Four participants also performed a standard retinotopic mapping experiment with checkerboard stimuli for the purpose of outlining V1. Participants fixated a central dot and passively viewed a rotating wedge. This wedge was filled with a flickering red and green checkerboard pattern and rotated clockwise. There were 8 rotation cycles per experiment, each lasting 64 seconds. The experiment entailed one run which lasted 576s and which started and ended with 12 s of fixation.

Object polar angle mapping

The purpose of the object polar angle mapping experiment was to investigate whether object-selective ventral stream areas respond consistently to changes in the angle of different stimulus classes. Participants performed a one-back memory task while viewing pictures of faces, houses, tools or Fourier-scrambled stimuli. Pictures rotated clockwise (CW) or counterclockwise (CCW) in different runs. At random times, a stimulus was repeated and participants had to indicate the repetition with a button press. Repetitions occurred 15 to 25 times per run. Each stimulus consisted of four simultaneously presented identical pictures that were arranged along a virtual line of a certain angle (see **Figure 3.1A**). We chose the size and arrangement of pictures on the basis of subjective impressions of visibility during the pilot testing phase, as well as on the basis of practical considerations (i.e., how the four pictures could be fitted next to each other). For

both the polar angle and the eccentricity experiment with object stimuli we did not assume any specific formula for a cortical magnification factor, as such a formula exists only for early visual areas (Daniel & Whitteridge, 1961; Smith, Singh, Williams, & Greenlee, 2001). The first stimulus wedge appeared along the lower vertical meridian (6 o'clock position). Successive stimulus wedges appeared at an angle shifted in clockwise or counter clockwise directions, respectively. A cycle was completed when the wedge had travelled 360° back to the starting position. One run comprised six cycles of 64s and in each cycle 96 pictures (stimulus wedges) were presented. Each run started and ended with 12 s of fixation and lasted 408 seconds in total. Pictures were randomly drawn from an image pool of 24 faces, 24 houses, and 24 tools and 24 scrambled versions of faces, houses, and tools. The tool pictures were the same as in the object localizer. The face pictures were collected from the Face Recognition Data, University of Essex, UK. The house pictures were selected from the internet. Each stimulus was shown for 500 ms with an inter-stimulus interval (ISI) of 167 ms. Since the lower part of the screen was partially occluded by the MR coil, we shifted the center of the presentation such that it was located at 5.5° below the upper edge of the screen. The background color of the screen was grey.

Participants were instructed to keep their eyes fixated at the central fixation dot, which was present throughout the entire experiment, and to refrain from making eye movements. We told participants that maintaining fixation was more important than performing well on the 1-back task.

Object eccentricity mapping

Similar to the object polar angle mapping experiment, the object eccentricity mapping experiment was intended to probe neural sensitivity to changes in the eccentricity of visual

stimuli. Timing and participants' task were the same as in the object polar angle mapping experiment. The arrangement of pictures, however, was different. Here, each stimulus presentation consisted of one picture that was replicated 8 times and arranged circularly around the central fixation dot (**Figure 3.1B**). Successive pictures appeared at more central (contracting condition; CON) or more peripheral (expanding condition; EXP) locations, respectively. The distances between the center of the pictures and the central fixation dot ranged from 1.5° to 5.3°. One cycle was completed when the stimulus annulus had moved from the most central eccentricity (1.5° between fixation dot and center of pictures) to the most peripheral eccentricity (5.3° between fixation dot and center of pictures), or vice versa.

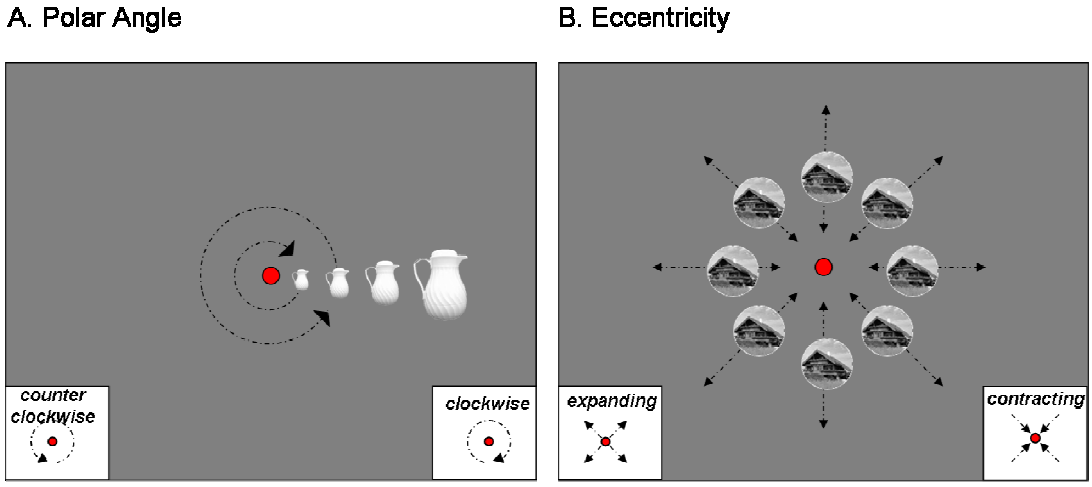

Figure 3.1: Stimulus presentation. A. Polar angle mapper with one exemplary polar angle and stimulus type (tools). In each run the stimulus wedge rotated only in clockwise or in counter clockwise directions. Only one stimulus class (e.g., tools) was used for one run. B. Eccentricity mapper with one exemplary eccentricity and stimulus type (houses). In different runs the stimulus ring either expanded or contracted. Also here only one stimulus class was used within a run.

Data Acquisition

Scanning was performed with a 4T Bruker MedSpec Biospin MR scanner and an 8-channel birdcage head coil. Functional images were acquired with a T2*-weighted gradient-recalled echo-planar imaging (EPI) sequence (TR = 2 s; TE = 33 ms; flip angle = 73°). We acquired 22 nearly axial slices, covering most of the temporal cortex and part of the occipital cortex (voxel resolution 2x2x2 mm). To account for distortions from magnetic field inhomogeneities, we performed a B0 correction based on a field mapping scan. We also performed a high-resolution (1 x 1 x 1 mm^3) T1-weighted 3D MPRAGE anatomical sequence (sagittal slice orientation, image matrix = 256 x 224, FoV = 256 mm x 224 mm, 176 partitions with 1 mm thickness, GRAPPA acquisition with acceleration factor = 2, duration = 5.36 min, TR = 2700, TE = 4.18, TI = 1020 ms, 7° flip angle) for each participant.

Data Analysis

Data were analyzed with Brain Voyager QX version 2.1 (Brain Innovation, Maastricht, The Netherlands) and Matlab 7.3 (The MathWorks, Inc., USA). Preprocessing followed standard procedures (Goebel, Esposito, & Formisano, 2006). We discarded the first three volumes of each functional scan. Preprocessing of the functional data included slice scan time correction (cubic spline interpolation), 3D motion correction (trilinear/ sinc interpolation) and high-pass temporal filtering (GLM with Fourier basis set with 2 cycles). Each functional scan was then co-registered to the de-skulled anatomy in native space of each participant. The co-registered functional and anatomical scans were then transformed into a standardized (Talairach & Tournoux, 1988) space.

ROI selection

The object localizer experiment was analyzed with the General Linear Model. Blocks of stimulation were modeled as a box car function, which was convolved with a dual gamma hemodynamic response function (this applies to all analyses of this study). Contrast analyses were performed to determine regions of interest (ROIs). FFA was determined by contrasting faces with houses, tools, and scrambled pictures. Similarly, PPA was determined with the contrast houses versus faces, tools and scrambled pictures. The resulting parameter maps were used to outline the two ROIs. The parameter maps were generally thresholded at a false discovery rate (FDR) (Genovese et al., 2002) of $q < 0.05$. For outlining the left FFA of one participant the threshold was raised ($p<0.00004$) in order to separate FFA from OFA. We identified FFA and PPA in all participants and in all hemispheres (**Table 2.1** for the mean Talairach coordinates **Table 5.1** in the appendix for all coordinates and sizes).

For the localization of V1 we applied a lag correlation analysis to the standard retinotopic mapping data (see the following section "Lag correlation analysis"). The resulting functional data were projected on the flattened surfaces of the brain. V1 was defined as the area from the calcarine sulcus up to the first inversion of the field sign (Sereno et al., 1995).

Lag correlation analysis

A lag correlation analysis exploits the fact that the stimulus presentation follows a fixed temporal and spatial order. We modeled a regressor with a box-car at each cycle onset and convolved the entire modeled time course with a hemodynamic response function. For each voxel, we calculated the correlation between this regressor and the BOLD time course. Since each stimulus presentation within a cycle had a constant offset with respect to the cycle onset, we could shift

our regressor for the time lag of one signal acquisition (one TR or 2 s) and re-compute the correlation with the BOLD time course. This procedure was repeated for 32 lags (32 TRs), i.e., for one full cycle of 64 s. For each voxel we subsequently selected the lag value that yielded the highest correlation. Since a particular lag corresponded to a particular angle or a particular eccentricity, this procedure allowed us to infer a voxel's preferred angle and eccentricity. In this way we assigned to each voxel a preferred visual field (VF) location. In order to reduce the impact of noise we excluded voxels whose preferred VF location in CCW and CW (EXP and CON) runs differed by more than 8 lags, which is equivalent to one quadrant (polar angle experiment) or 0.95° radius (eccentricity experiment). For the remaining voxels we averaged the lag and correlation values of CCW and CW runs and of EXP and CON runs, respectively. The resulting data were, unless stated otherwise, thresholded at $r > 0.15$, which corresponds to $p < 0.05$. Thus, our definition of a space-sensitive voxel requires that a voxel's BOLD signal time course is significantly correlated with at least one of our 32 lagged regressors, each of which represents one specific angle or eccentricity.

3.3 Results

Localization of FFA and PPA.

We used the object localizer experiment to outline FFA and PPA. FFA was defined as the continuous voxels in the fusiform gyrus that were more activated to faces than to houses, objects and scrambled pictures. Similarly, PPA was defined as the voxels in the parahippocampal gyrus that were more activated to houses than to faces, objects and scrambled pictures. We localized FFA and PPA in both hemispheres of all participants. Error! Reference source not found. lists the means and the standard deviations of the x, y and z coordinates of all participants. A complete table of individual coordinates and sizes of ROIs can be found in the Appendix, **Table 5.1**.

Table 3.1: Mean Talairach coordinates for FFA and PPA, derived from all 8 participants in the localizer experiment.

	Left			Right		
	X	Y	Z	X	Y	Z
FFA	-38 ± 2.6	-49 ± 10	-15 ± 3.5	36 ± 2.35	-47 ± 5.3	-15 ± 3.1
PPA	-26 ± 1.7	-42 ± 5.3	-9.6 ± 2.6	25 ± 2.5	-44 ± 6.2	-8.1 ± 2.3

Values represent the mean ± std in mm.

Polar angle and eccentricity maps in FFA and PPA. The lag correlation analysis of the object polar angle and eccentricity experiments yielded lag maps as shown on the inflated cortical surface of one exemplary participant (**Figure 3.2**). Each color in these lag maps represents a particular polar angle or eccentricity. The polar angle maps indicate that left ROIs predominantly represent the right VF, while the right ROIs prefer the left VF. By closer inspection, however, one can detect some patches that represent the ipsilateral VF, especially in the right ROIs. Notice

that almost the entire areas of FFA and PPA are sensitive to the polar angle of stimuli, as can be seen by the presence of a color. Patches that are not colored in these maps reflect areas that did not have a significant correlation with any VF location.

The eccentricity maps demonstrate that FFA has a detailed representation of eccentricity, as indicated by the presence of various colors from legend. In contrast, PPA demonstrates mainly peripheral eccentricities, which are represented by blue and green. The eccentricity maps are patchier than the polar angle maps, which implies that FFA and PPA are more sensitive to the polar angle than to the eccentricity of stimuli. This issue will be investigated in the paragraph The extent of space sensitivity in FFA and PPA**.**

The following paragraph addresses in more detail which VF locations are represented by individual voxels.

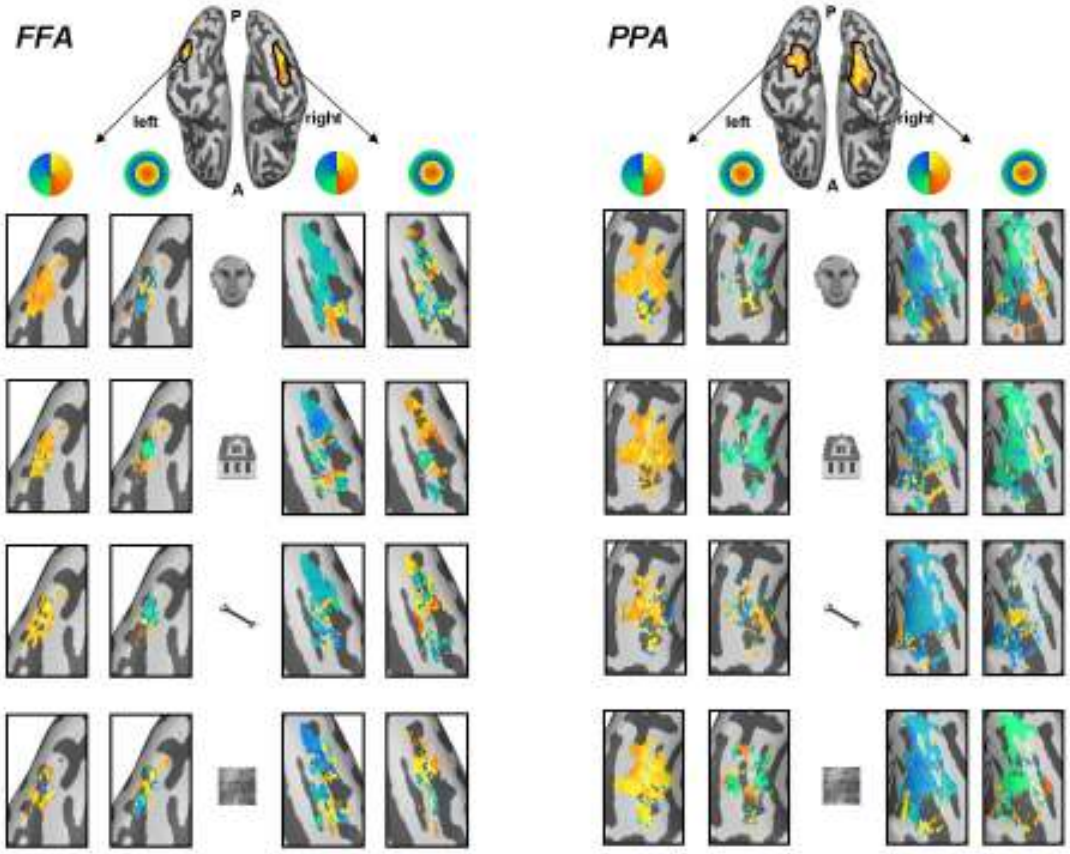

Figure 3.2: Polar angle and eccentricity maps in FFA and PPA of one participant and for the four stimulus categories faces, houses, tools and scrambled objects. Shown is the ventral surface of the brain. The colors of the maps refer to the preferred location in the visual field, as indicated by the two circular color legends for polar angle and eccentricity at the top of the figure. Colors from red to yellow code for the right (polar angle) and central (eccentricity) VF field, and colors from blue to green code for the left and peripheral VF. Regions that are not colored represent voxels whose time course did not yield significant correlations with the model HRF at any lag. A= anterior, P= posterior. Maps are thresholded at r > 0.15.

Distribution of preferred VF locations. In order to get a better overview of the distribution of preferred VF locations of individual voxels we looked at the data within a given ROI independently of the anatomical position of voxels. For this purpose we show the preferred angle and eccentricity of each voxel in polar plots (**Figure 3.3**), where each dot represents the preferred VF location of one voxel. The lag values which were obtained in the polar angle

mapping experiment were transformed into polar angle values from 0° to 360°, whereas the lag values from the eccentricity experiment are plotted in the original values, that is, from 1.5° to 5.3° visual angle. Note that in the eccentricity mapping experiment the smallest eccentricity was not foveal, because stimuli were always presented within a ring that comprised 8 identical pictures. The smallest distance between the central fixation cross and the center of the stimulus ring was 1.5°.

The distribution of preferred VF locations in FFA is characterized by some clustering around the central and contralateral VF, but various other eccentricities and ipsilateral VF locations are also covered. In PPA there is an even more homogenous distribution of voxel preferences across the visual field. We calculated an index for the contralateral VF bias with the formula

$$VFB = \frac{vox_{contra} - vox_{ipsi}}{vox_{contra} + vox_{ipsi}} \qquad \textbf{(1)}$$

where VFB is the visual field bias, vox_{contra} is the percentage of voxels with contralateral preference, and vox_{contra} is the percentage of voxels with ipsilateral preference. The values range from -1 to 1, with negative values indicating an ipsilateral visual field bias, 0 indicating no bias, and positive values indicating a contralateral bias. Since the surface maps in **Figure 3.2** raised the impression that the right hemisphere ROIs have more ipsilateral VF preferences than left hemisphere ROIs, we calculated the contralateral bias separately for each hemisphere. **Figure 3.4** shows that FFA and PPA have, as expected, a contralateral VF bias (mean index of left FFA: 0.6 (standard deviation 0.28), right FFA 0.22 (0.48), left PPA 0.41 (0.43):, right PPA: 0.44 (0.34)). We tested the resulting VF bias against the null hypothesis that there is no bias by

computing one-sample t-tests of the VF bias indices. Left FFA has a significant contralateral VF bias ($t(7) = 10.847$, $p = 0.000$), while right FFA does not ($t(7) = 1.835$, $p = 0.109$; all t-test results are two-tailed). PPA in both hemispheres has a significant contralateral bias (left PPA: $t(7) = 4.497$, $p = 0.003$; right PPA: $t(7) = 5.163$, $p = 0.001$).

Since substantial research has been conducted on spatial sensitivity in V1, we analyzed the VF bias in V1 in order to have a reference for our results in FFA and PPA. V1 had a slightly stronger contralateral VF bias than FFA and PPA (left V1: mean (std) = 0.73 (0.12), right V1: mean = 0.56 (0.13)). However, the difference of VF biases between V1 and FFA and PPA was not significant (left hemisphere: $t(3) = 0.818$, $p = 0.473$; right hemisphere: $t(3) = 0.717$, $p = 0.525$; t-tests comparing the VF bias in V1 with the mean VF bias of FFA and PPA). The values in left and right V1 were both significantly different from zero (left V1: $t(3) = 54.287$, $p = 0.000$; right V1: $t(3) = 11.246$, $p = 0.002$). Since FFA and V1 had different bias values in the left and right hemispheres, we conducted further analyses in which we compared the two hemispheres. We tested for hemispheric differences of VF bias in different visual areas by conducting a repeated measures ANOVA on VFB with factors ROI (FFA, PPA) and hemisphere (left, right). (Since we defined V1 in only four participants, we analyzed FFA and PPA separately from V1.) There was no overall effect of hemisphere ($F(1,7) = 1.905$; $p = 0.21$), but there was an interaction of hemisphere and ROI ($F(1,7) = 7.086$; $p = 0.032$). A paired-samples t-test in FFA confirmed that left FFA had indeed a stronger contralateral bias than the right FFA ($t(7) = 2.386$; $p = 0.048$). PPA did not show any difference between hemispheres ($t(7) = -0.194$; $p = 0.852$). V1 showed a trend for an effect of hemisphere ($t(3) = 2.419$, $p = 0.094$).

We also checked for any biases with respect to the upper and lower visual field by applying the analogous formula to **equation (1)**.We found a weak lower VF bias in FFA (left

FFA: mean = -0.04 (std 0.34), right FFA: mean = -0.15 (0.35)). These indices were not significantly different from zero (left FFA: $t(7) = -0.519$, $p = 0.62$; right FFA: $t(7) = -1.796$, $p = 0.116$). PPA showed an upper VF bias in the left hemisphere (left PPA: mean = 0.23 (0.3); $t(7) = 4.242$, $p = 0.004$) but not in the right hemisphere (right PPA: mean = 0.03 (0.32), $t(7) = 0.526$, $p = 0.615$). In comparison, ventral V1 had a strong upper VF bias (left ventral V1: mean = 0.67 (0.18), $t(3) = 8.171$, $p = 0.004$; right ventral V1: mean = 0.58 (0.14), $t(3) = 12.04$, $p = 0.001$) and dorsal V1 had a lower VF bias (left dorsal V1: mean = -0.57 (0.21), $t(3) = -8.94$, $p = 0.003$; right dorsal V1: mean = -0.56 (0.18), $t(3) = -8.25$, $p = 0.004$).

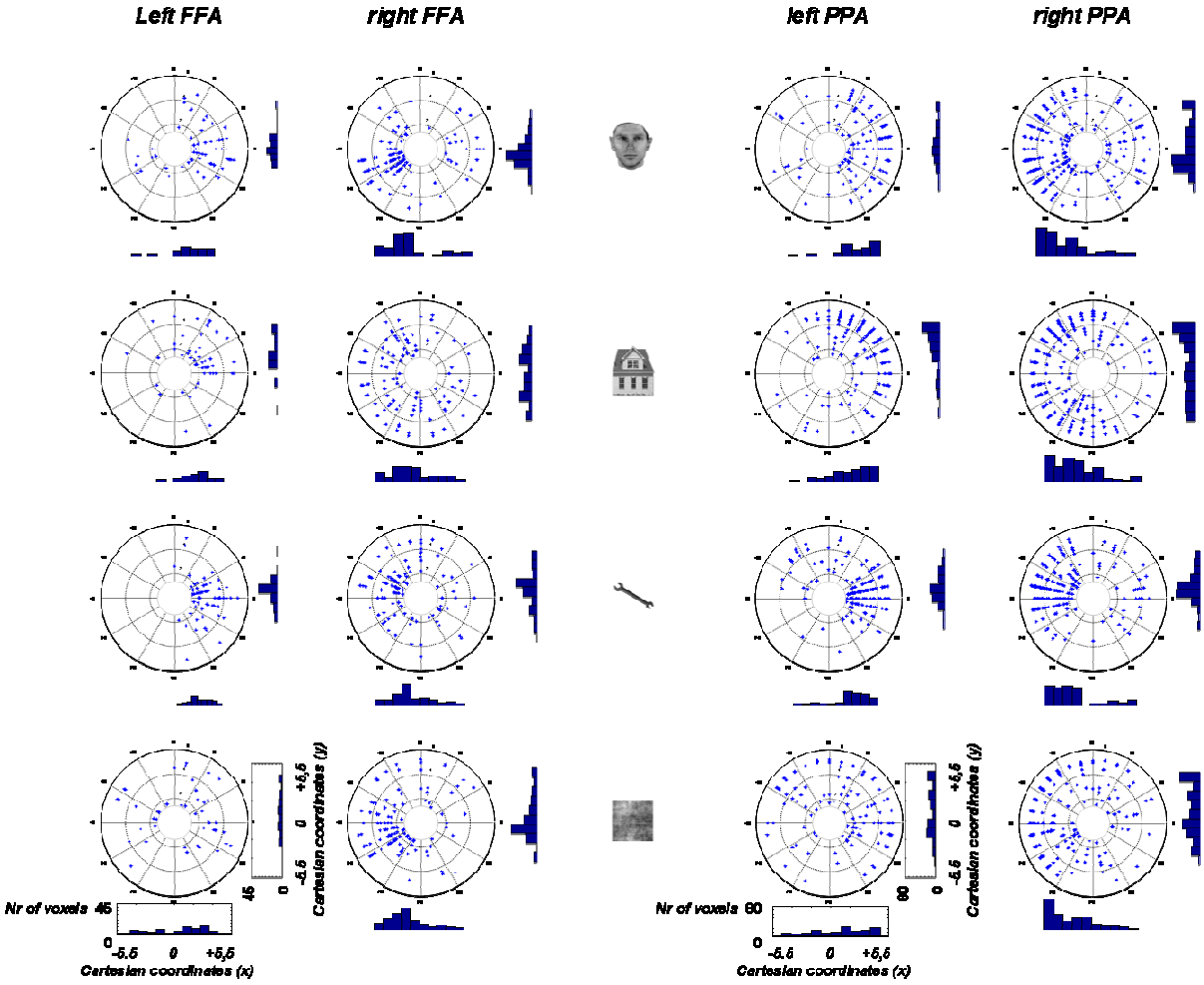

Figure 3.3: **Distribution of preferred VF locations in FFA and PPA of one participant. Each blue dot represents the preferred polar angle and eccentricity of one voxel. The values for eccentricity range from 1.5° visual angle to 5.3° visual angle; the white circle in the center of each polar plot indicates the visual field area where no stimuli were shown. The lag values for the polar angle were transformed into angular values for this plot. The histograms at the bottom and right side of each polar plot summarize the number of voxels at certains VF location separately for the horizontal (bottom histograms) and vertical (right side histograms) aspects of the VF. For FFA the number of voxels (y-axis) ranges from 0 to 45 voxels, for PPA it ranges from 0 to 80 voxels.**

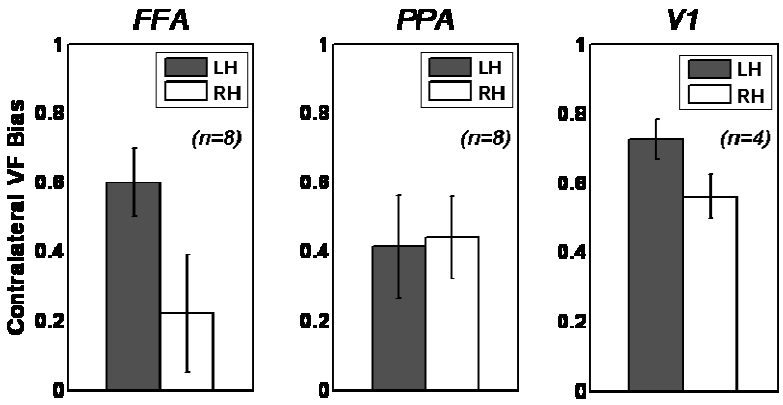

Figure 3.4: **Contralateral VF bias for regions FFA and PPA and V1. The contralateral bias is stronger in left FFA and V1 than in right FFA and V1. Data for FFA and PPA are based on 8 participants, for V1 on 4 participants (standard retinotopic mapping data for defining V1 existed only for 4 participants). Error bars are standard errors of the mean between subjects. Values range from 0 (no bias) to 1 (maximum contralateral VF bias).**

The extent of space sensitivity in FFA and PPA. According to our definition of space sensitivity, we found that a large percentage of voxels in FFA and PPA are space-sensitive (**Figure 3.5**). The percentage of space-sensitive voxels refers to the fraction of space-sensitive voxels from the total number of voxels as defined in the separate localizer experiment. On average (across 8 participants and collapsed over faces, houses, objects and scrambled objects) 62% of voxels in FFA are sensitive to angle and 42% are sensitive to eccentricity. In PPA 63% of voxels are sensitive to angle and 47% to eccentricity. In comparison, V1 (n = 4), which is assumed to be highly space-sensitive, had 74% (polar angle) and 63% (eccentricity) of space-sensitive voxels. We inspected where the space-sensitive voxels were located within the regions of interest. There was some clustering of space-sensitive voxels and of space-insensitive voxels, but both types of voxels were distributed throughout the ROIs (**Figure 3.6**).

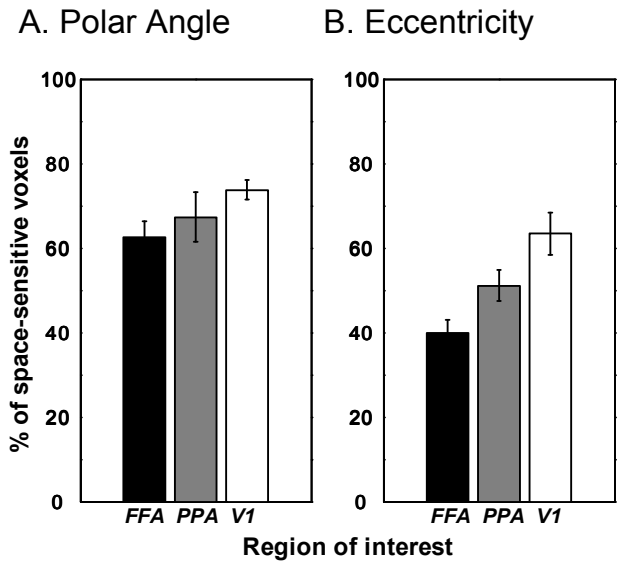

Figure 3.5: **Percentage of space-sensitive voxels from original ROI. Panel A: percentage of voxels that are sensitive to polar angle; panel B: percentage of voxels that are sensitive to eccentricity. The requirements of being space-sensitive are a) that preferred VF locations in CW and CCW or in EXP and CON are not further apart than one quadrant or 0.95° radius, and b) that the maximum correlation is at least r = 0.15. FFA and PPA: n = 8; V1: n = 4.**

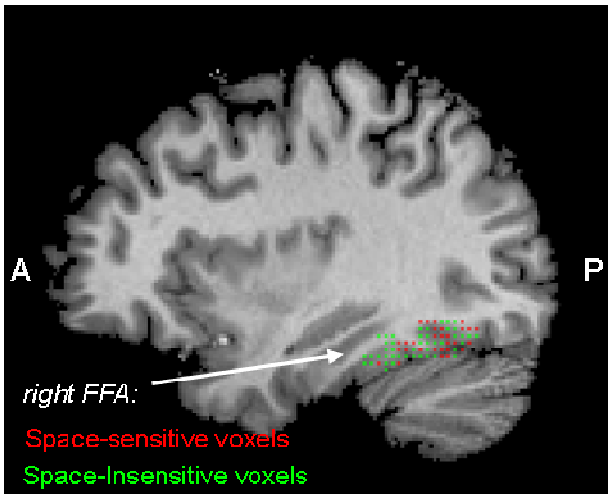

Figure 3.6: **The cortical location of space-sensitive and space-insensitive voxels of one participant's right FFA. Space-sensitive voxels (in red) are spread between space-insensitive voxels (in green), but they cluster loosely together. Colored dots represent the centroids of voxels. A = anterior, P = posterior.**

Interaction of space and category sensitivity.

So far we have reported results pertaining to space sensitivity of FFA and PPA in general, and have left aside any potential differences between the four stimulus classes. We analyzed our data in two different ways to address the question of dependency between space and category representations. First, we computed the percentage of space-sensitive voxels separately for the preferred and the non-preferred stimulus classes. Second, we computed the category selectivity of space-sensitive voxels and looked whether the extent of category selectivity depends on the extent of space sensitivity.

For the first analysis, we assigned to FFA and PPA a preferred stimulus class (faces for FFA and houses for PPA, based on the maximum response of each in the localizer experiment) and three non-preferred stimulus classes (houses, tools and scrambled objects for FFA and faces, tools and scrambled objects for PPA). We calculated the percentage of space-sensitive voxels separately for the preferred stimulus class and for the mean of the three non-preferred stimulus classes (**Figure 3.7)**. 67.12% of FFA voxels showed sensitivity to the angle of the preferred stimulus class and 60.78% showed sensitivity to the angle of the non-preferred stimulus classes. In PPA there were 63.73% and 63.00% of polar angle-sensitive voxels for the preferred and non-preferred classes, respectively. For eccentricity the mean percentages of space-sensitive voxels for preferred and non-preferred stimuli in FFA were 40.41 and 41.85, respectively, and in PPA they were 50.82 and 45.74, respectively. We tested whether the two ROIs showed different effects of category preference and spatial dimension in terms of number of spatially selective voxels. To this aim, we computed an ANOVA on the percentage of space-sensitivie voxels with the factors spatial dimension (polar angle, eccentricity), category (preferred, non-preferred) and ROI (FFA, PPA). This analysis revealed a nearly significant three-way interaction of spatial

dimension, category and ROI ($F_{1,7}$=5.49; p = 0.052), indicating that category preference affects space sensitivity differently for polar angle and eccentricity. We tested this further by computing two ANOVAs separately for the two spatial dimensions. For eccentricity we found a significant interaction of ROI and category ($F_{1,7}$=8.661, p=0.022). This interaction was not present for polar angle ($F_{1,7}$=1.769, p=0.225). Finally, we looked at the effect of category preference on the number of space-sensitive voxels separately for each ROI. A paired-samples t-tests revealed that in the polar angle experiment there were more space-sensitive voxels in FFA when the preferred stimulus class was shown than when the non-preferred stimulus classes were shown (t(7) = 3.742, p = 0.007). In PPA this effect was not significant (t(7) = 0.82, p = 0.429). The difference between preferred and non-preferred stimuli for eccentricity was significant for PPA (t(7) = 2.526, p = 0.039), but not for FFA (t(7) = -0.047, p = 0.964).

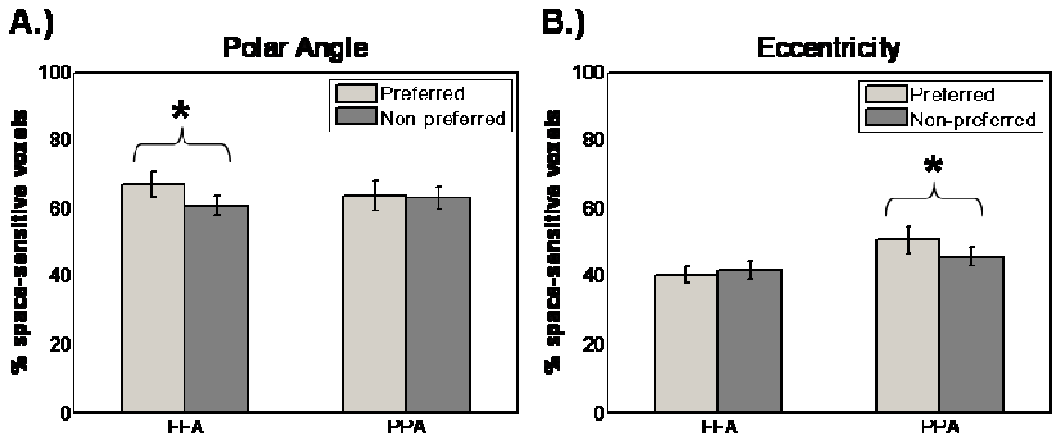

Figure 3.7: **Percentage of space-sensitive voxels as a function of preferred and non-preferred stimulus class. The percentage of space-sensitive voxels is the fraction of voxels from the localizer voxels that exhibits space sensitivity in a particular run (e.g., polar angle and face stimuli). The preferred stimulus class for FFA is faces, the non-preferred stimulus classes are houses, tools and scrambled objects. For PPA the preferred stimulus is houses, the non-preferred stimuli are faces, tools and scrambled objects. A.) Percentages of polar angle-sensitive voxels. FFA has significantly more space-sensitive voxels for the preferred than for the non-preferred stimulus classes. There is no difference in PPA. B.) Percentages of eccentricity-sensitive voxels. There are more space-sensitive voxels in PPA for the preferred than the non-preferred stimulus classes. For FFA the difference is not significant. See text for details.**

Second, we examined the activation strength of space-sensitive voxels to different stimulus classes and calculated the category selectivity of these voxels. We could not analyze the strength of activation in the object retinotopic mapping experiment, because there was no fixation condition that would serve as a baseline. We therefore used our definition of space-sensitive voxels from the object retinotopic mapping experiment and calculated a GLM on the data from the object localizer experiment. That is, we divided the original ROIs into two sub-ROIs, the space-sensitive FFA/ PPA and the space-insensitive FFA/ PPA and obtained beta weights for each. The results are shown in **Figure 3.8**. Space-sensitive voxels are similarly category-selective as the space-insensitive voxels. Activation is strongest for faces in the FFA sub-ROIs and strongest for houses in the PPA sub-ROIs.

We looked closer at the differences in category selectivity of space-sensitive and space-insensitive voxels by computing a category selectivity index for each. Space-sensitive voxels had a slightly lower index than space-insensitive voxels (3.17 versus 3.67; FFA and PPA averaged), but the difference was not significant (paired-samples t-test, $t(7) = -1.385$, $p = 0.208$). Thus, there is a tendency that space-sensitive voxels are less category-selective than are space-insensitive voxels. Might this effect become more apparent if we apply a stricter criterion for being "space-sensitive", that is, if we raise the threshold when defining space-sensitive voxels? We re-distributed the sub-ROIs according to the thresholds $r = 0.05$, 0.10, 0.15 (corresponds to $p > 0.05$ and is used for all other analyses), 0.20, 0.25, and 0.30. Raising the threshold in this way corresponds to decreasing the number of space-sensitive voxels and increasing the number of space-insensitive voxels, because increasingly less voxels are labeled "space-sensitive" and accordingly remain in the pool of "space-insensitive" voxels. In other words, the higher the threshold, the more robustly the label "space-sensitive" applies to the remaining space-sensitive

voxels. For each new distribution we obtained beta weights and calculated the category selectivity index for both sub-ROIs. The resulting values indicate that category selectivity indeed goes down when space sensitivity increases (**Figure 3.9**). For very high thresholds (r = 0.25 and r = 0.30) the difference between space-sensitive (blue line) and space-insensitive (green line) voxels was significant (for r = 0.25: t(7) =-2.469, p = 0.043; for r=0.30: t(7) = -2.387, p = 0.048; paired-samples t-test (two-tailed)).

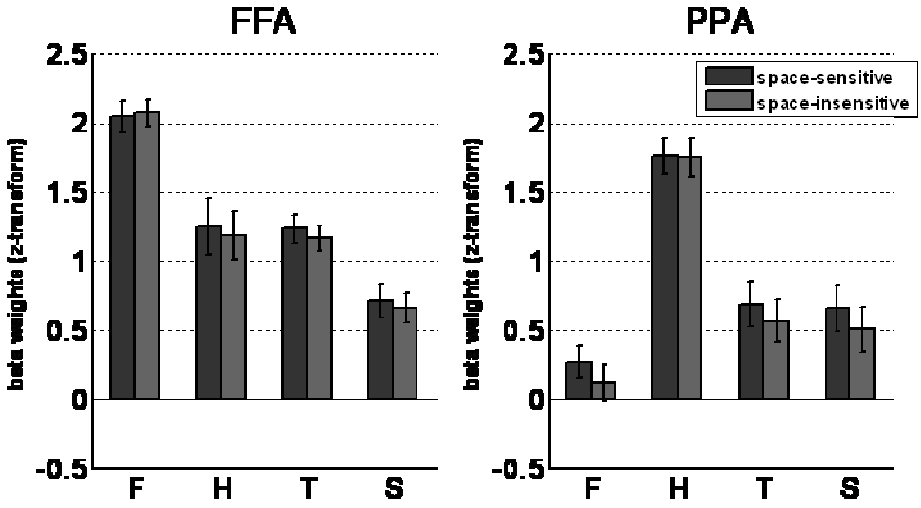

Figure 3.8: **Mean beta weights (n = 8) of space-sensitive and space-insensitive FFA and PPA voxels for four stimulus classes. Data are based on the separate localizer experiment in which pictures of faces (F), houses (H), tools (T) and scrambled objects (S) were presented in the center of the screen. Error bars are standard errors between participants.**

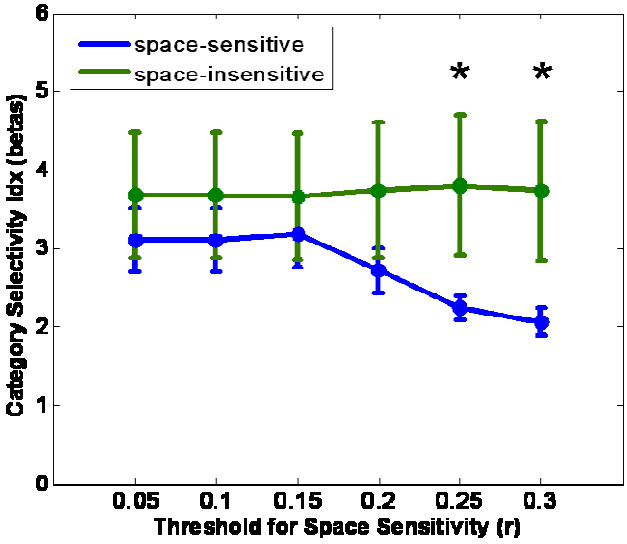

Figure 3.9: Category selectivity decreases when space sensitivity increases. Space-sensitive voxels have a lower category selectivity index than space-insensitive voxels, and it decreases even more when the threshold for defining space sensitivity becomes stricter. Asterisk indicates a significant difference of the category selectivity index between space-sensitive and space-insensitive voxels (paired-samples t-test). Category selectivity index was computed as *beta(preferred category)/mean(betas (non-preferred categories))*. N=8.

Selectivity for VF locations.

Our analyses are based on the peak response of voxels. It might be, however, that voxels have more than one preferred VF location. In other words, there could be a maximal response to one VF location, and a smaller yet significant response to another VF location. If this were the case, then our analyses might have omitted an important characteristic of space encoding in ventral stream areas. In Figure 3.10we plot the correlation values between the actual and the predicted activation time courses for each of the 32 lags in our experiment. Shown are the correlations of all FFA and PPA voxels of one representative participant for the expanding faces experiment. The lags are plotted on the x-axis, where the lag corresponding to the highest correlation value, and therefore the lag representing the preferred VF location according to our definition, is plotted in the middle of the axis (marked as 'peak'). We centered the lag values thus because different

voxels have different lag values associated with the maximum correlation, and accordingly a plot with a fixed x-axis ranging from 1 to 32 could not give a clear picture of the tuning of all voxels. Most voxels shown in Error! Reference source not found. have a significant peak in the correlation values, and the majority appears to have only one significant peak. Significant correlation values are above 0.15 and are indicated by the blue horizontal line.

In order to get a more general estimate of space selectivity in our data set we counted the peaks of activation time courses across all subjects and all experimental conditions. Because of the sluggishness of the hemodynamic response we considered peaks that are less than 8 seconds apart from each other as one peak. The mean number of peaks across all participants is shown in **Figure 3.11**. The mean across participants is based on the average number of peaks across all voxels in an area and across 16 experimental runs (CCW, CW, EXP and CON for faces, houses, tools, and scrambled objects). On average 901 voxels in the left FFA had at least one significant peak in their activation time course. This number dropped to 245 voxels having two significant peaks, which is a reduction of 73%. Only 28 voxels had three peaks, which is a reduction of 97% compared with the number of voxels having one peak. Finally, only one voxel had four peaks. In right FFA there were on average 542 voxels with one peak, and this number was reduced by 74% and 97% for two and three peaks, respectively. Similar reductions in the number of voxels were observed in left PPA (two peaks: 74%, three peaks: 97%, four peaks: 99.9%) and right PPA (two peaks: 77%, three peaks: 98%).

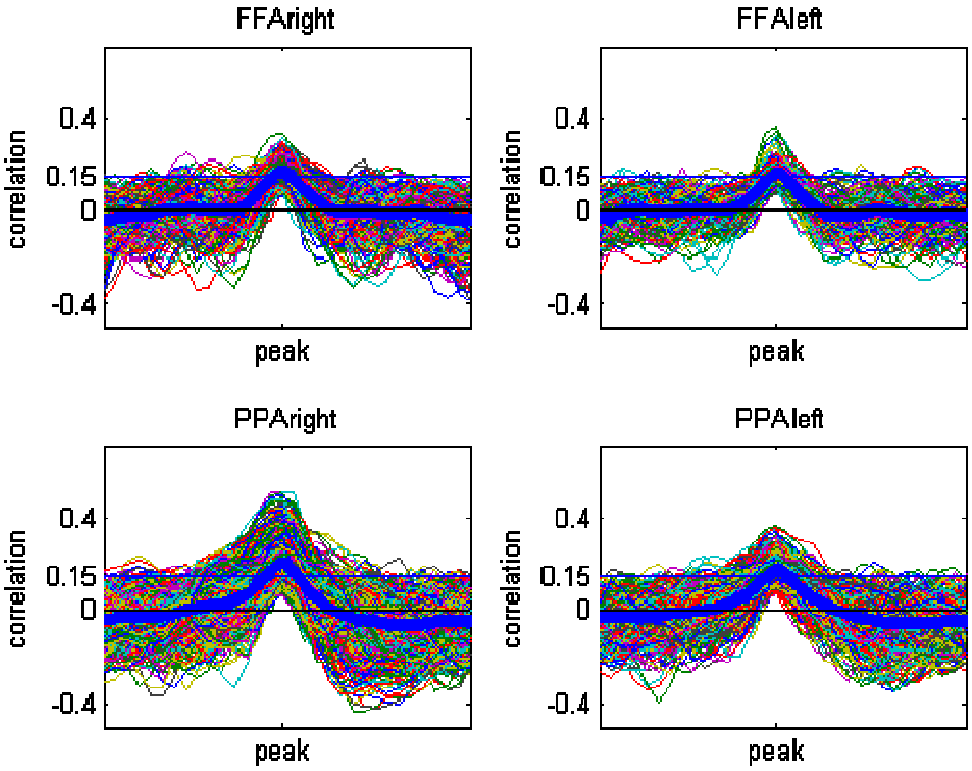

Figure 3.10: Correlations between voxel time course and predicted time course at 32 time points (lags). Shown is one representative participant (P1) and run (faces, EXP). The four panels show the correlation values of all voxels in left and right FFA and PPA. Each line in a panel represents one voxel. The blue bold line is the mean correlation of the correlation values of all voxels within an area. The x-axis depicts the 32 lag values, and the lags corresponding to the highest correlation (peak) of each voxel are aligned in the middle of the axis. The y-axis represents the correlation between the voxel time courses and the model regressor. Significant activation is reflected by a correlation of r > 0.15 (indicated by the blue horizontal line). Notice that the majority of voxels has only one significant peak in the activation time course.

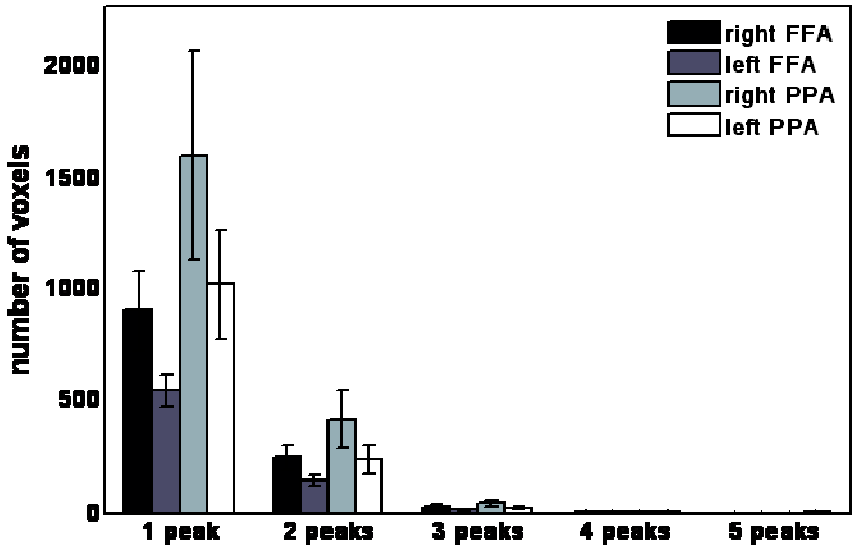

Figure 3.11: Number of peaks in the correlation profile of FFA and PPA voxels. The graph depicts how many voxels (y-axis) have one or more peaks (x-axis). The bars reflect the group mean (n = 8) of each participant's average number of peaks across all 16 experimental runs (faces, houses, tools, scrambled pictures; CCW, CW, EXP, and CON). Error bars refer to the standard error of the group mean. The majority of voxels have only one activation peak, indicating that ventral stream neurons have a high selectivity for one visual field location.

3.4 Discussion

Spatial sensitivity in FFA and PPA

We have used a combination of a retinotopic mapping design and object stimuli to demonstrate sensitivity to polar angle and eccentricity in FFA and PPA. We found polar angle and eccentricity maps in FFA and PPA in all eight tested participants. The polar angle maps were dominated by a contralateral VF representation, which is in line with a previously reported contralateral VF bias in high-level areas (Hemond et al., 2007). The right hemisphere maps also contained voxels which encoded the ipsilateral hemifield. In many maps voxels coding for the ipsilateral VF were located in the anterior parts of the ROIs. This finding goes along with the hypothesis that the further anterior one looks at the ventral stream, the more size-invariant is the representation of visual objects (Konen & Kastner, 2008; Kovács, Cziraki, Vidnyánszky, Schweinberger, & Greenlee, 2008). The first instance of the ventral stream (and of the dorsal stream), V1, is highly specific to the location and low-level features of visual stimuli (Hubel & Wiesel, 1968). At each processing level further up the ventral stream, the representation of visual stimuli becomes more abstract. LO, an area at the border between early visual areas and high-level face- and house-selective areas, is selective to object categories, but it is also highly sensitive to the location of stimuli (Sayres & Grill-Spector, 2008). The next anatomical step along the ventral stream is FFA, which in our study shows a mixed behavior with respect to VF biases. The left FFA is more similar to early visual areas and LO in that it has a strong contralateral VF bias. The right FFA, on the other hand, has a more complete VF representation, which as a net response looks like location invariance. PPA, which generally lies anterior and

medial of FFA, has a broad representation of the VF in both hemispheres. Again, the net response of PPA should accordingly be invariant to changes in the location of stimuli. Such invariance was reported for viewpoint in Ewbank et al. (Ewbank et al., 2005). Our results suggest that while the net response of PPA might appear invariant to location, the underlying voxel-wise representation of space is highly selective for specific VF locations. Thus, previous findings of location-invariance in high-level object-selective areas can be explained by the fact that these studies have looked at the mean response of the areas as whole. We show here that a voxel-based analysis reveals that information about space is preserved even in medial ventral areas FFA and PPA. Interestingly, we found that also V1 has a weaker contralateral VF bias in the right than in the left hemisphere. V1 is assumed to have a strong contralateral VF bias, which in fact is the reason why the retinotopic mapping of early visual areas, including V1, is based on an analysis that only considers contralateral stimulation (Sereno et al., 1995). However, it has been reported that V1 encodes also the ipsilateral VF field to some extent (Dumoulin & Wandell, 2008; Tootell, Mendola, Hadjikhani, Liu, & Dale, 1998). What could be the reason for the differences in the hemifield bias between hemispheres? The right hemisphere has long been regarded as the more dominant hemisphere in attentional processes (Heilman & Abell, 1980; Mesulam, 1999). The main indication for this assumption comes from the observation that patients exhibit cognitive deficits predominantly after right hemisphere strokes. The phenomenon of left hemifield neglect has been attributed to the unilateral representation of space in the left hemisphere and the bilateral representation of space in the right hemisphere. If the right hemisphere is affected by a stroke, only the left hemisphere can process spatial information and accordingly only the right side of space is represented in the brain. In contrast, if the left hemisphere is affected by a lesion, then the right hemifield is still partially represented, because

the right hemisphere processes information from both left and right hemifields. Our data fit well into this model: we found a strong contralateral VF bias in left FFA and V1, and a more bilateral VF representation in right FFA and V1. Interestingly, our results suggest that PPA does not comply with such hemispheric differences. Instead, PPA exhibited an equal level of contralateral VF bias in both hemispheres, which was intermediary between the levels in the left and right FFA and V1. The lack of differential processing of space in the left and right hemispheres might be explained by the fact that the angular aspect of visual stimuli is less important to PPA than the eccentric aspect, which will be discussed in the paragraph *Interaction of category and space.*

The representation of the vertical VF was largely balanced between upper and lower VF, as indicated by the low indices of the vertical VF bias. FFA had a non-significant trend to a lower VF bias, and PPA had a non-significant trend to an upper VF bias. These trends are in line with a study from Schwarzlose and colleagues (Schwarzlose et al., 2008), in which the researchers found similar biases in the activation strength of FFA and PPA when looking at average responses of these regions.

The eccentricity maps in our study showed less orderly arrangement than the polar angle maps. While PPA voxels predominantly represented the periphery, FFA voxels had a more complete representation of eccentricity. However, for both FFA and PPA voxels with similar eccentricity preferences were distributed throughout the ROI. Hasson et al. (Hasson, Levy, Behrmann, Hendler, & Malach, 2002) proposed eccentricity as an organizational principle of ventral stream areas, with more lateral areas, such as FFA, representing the central VF, and more medial areas, such as PPA, representing the periphery. In our study the net response of an area complies with this theory, but within an area we did not find a similar organization. In contrast, we found little

consistency in the organization of eccentricity maps, both between participants and between stimulus conditions. Furthermore, fewer voxels were sensitive to eccentricity than to polar angle (on average 62.5% of FFA and PPA voxels were sensitive to polar angle, but only 44.5% were sensitive to eccentricity). These facts might imply that for FFA and PPA the polar angle aspect carries more important information about the position of an object than the eccentric aspect. We compared the extent of sensitivity to polar angle and eccentricity in FFA and PPA to that in V1, since V1 has been shown to contain a full representation of the VF in both angular and eccentric coordinates (Sereno et al., 1995). One should therefore assume a high percentage of voxels in V1 to be space-sensitive. Our data did indicate a higher percentage of space-sensitive voxels in V1 than in FFA and PPA (74% for polar angle and 63% for eccentricity), but these percentages were far from 100%. There are at least two possible explanations for this discrepancy. On the one hand, it could be that our stimulation was not optimal. Alternatively, it might be that V1 is in fact not completely space-sensitive, and that the retinotopic maps that have been reported in various studies are based on a subset of V1 voxels (we are not aware of a study that explicitly states the percentage of space-sensitive voxels in V1). Irrespective of which of the two explanations is correct, we can say that FFA and PPA contain a high percentage of space-sensitive voxels and can thus hardly be considered to be space-invariant.

Interaction of category and space

Comparing space sensitivity for three object categories and for scrambled objects, we were able to demonstrate that a representation of space exists for any type of stimulus we employed, even for low-level scrambled pictures. The existence of spatial sensitivity maps irrespective of the type of stimulus suggests that category and space are coded independently of each other. It is

well-known, however, that face- and house-selective areas respond maximally, but not exclusively to their preferred stimulus class (Downing et al., 2006a) (and see our experiment 1). Accordingly we did not expect to find responses to changes in stimulus location exclusively for the preferred stimulus class. However, if space-sensitive voxels were also category-selective, we expected to find a larger number of space-sensitive voxels when the preferred stimulus class is shown. In contrast, if space and category were coded independently, there should be no difference in space-sensitivity between preferred and non-preferred stimulation conditions. We found mixed evidence for these two hypotheses. For polar angle FFA had the largest number of space-sensitive voxels for face stimuli. Similarly, PPA had the most space-sensitive voxels for houses in the eccentricity experiment. However, this dependence between number of voxels and category preference was not significant for PPA in the polar angle experiment and for FFA in the eccentricity experiment. The absence of an effect might be due to the relatively small number of participants. We scanned only eight participants, which might have been insufficient for the statistical assessment of small effects. On the other hand, it might be that an interaction of category and space in FFA is more relevant for polar angle, while it is more relevant for eccentricity in PPA. For PPA the importance of eccentricity has been proposed (Hasson et al., 2002). Hasson and colleagues have suggested that PPA is located in the medial part of the ventral temporal cortex because this part of the cortex predominantly responds to visual stimuli in the peripheral VF. In fact, these researchers have suggested that eccentricity biases in the processing of object categories are a general organizational principle of object-selective visual areas. We refine this theory by proposing that a) PPA encodes eccentricity preferentially for its preferred stimulus, namely, houses, and b) this category-dependent encoding of eccentricity is present in PPA but not in FFA.

To our knowledge, the importance of polar angle has not been discussed so far. Our data suggest that the polar angle of stimuli might be a crucial encoding aspect of object-selective areas. In fact, polar angle appears to be more important than eccentricity, since FFA and PPA were more sensitive to the polar angle than to eccentricity. In addition, FFA was more sensitive to the angular position of its preferred category than to the angular position of other categories. Finally, the polar angle maps showed more consistency than the eccentricity maps. The functional importance of polar angle as an organizational principle of object-selective areas is an interesting topic for future research.

We examined two types of voxels, space-sensitive and space-insensitive voxels, with regard to their selectivity for object category. To this means we analyzed the activation strength of each voxel type for four different stimulus classes. Both space-sensitive and space-insensitive voxels had the strongest activation for the preferred stimulus class, that is, for faces in FFA and for houses in PPA. This finding is not surprising, since all the voxels in question were originally defined as being more responsive to faces or houses, respectively. Interesting is, however, that the category selectivity index for space-sensitive voxels is slightly lower than that of space-insensitive voxels (3.17 versus 3.67). The difference between these values was not significant, but it does give the impression that the space-sensitive voxels care somewhat less about category than do the space-insensitive voxels. We therefore raised our criteria for space sensitivity in the main experiment by raising the threshold of the correlation between the modeled time course and the BOLD signal time course. Such a raise in threshold reduces the number of voxels that obtain the label “space-sensitive” but at the same time increases spatial specificity of the pool of voxels under consideration. This analysis revealed a clear dependency between the extent of space

sensitivity and the extent of category selectivity: the more space-sensitive are the voxels, the less they are category-selective. At high correlation thresholds the difference in category selectivity between space-sensitive and space-insenstive voxels became significant. These results imply two characteristics of object-selective areas. First, there is no strict separation of category and space into "category-selective" voxels and "space-sensitive" voxels. Rather, all voxels encode both aspects. Second, some voxels are more sensitive to category than to space, while other voxels are more sensitive to space than to category. The preferential encoding of one aspect comes at the cost of encoding the other aspect.

In sum, different types of analyses of our data suggest an interaction of category and space. A recent study by Kravitz and colleagues (Kravitz, Kriegeskorte, & Baker, 2010) found a similar dependency between category and space in object-selective areas. On the one hand, behavioral priming of object stimuli only led to increased recognition performance when the position of the stimuli remained unchanged. On the other hand, the activation pattern across voxels within object-selective areas showed lower correlations when stimuli appeared at different locations than when they remained at the same location. Thus, different experimental methods converge on the same findings: a) object-selective cortex is highly sensitive to space, and b) the representation of category is constrained by the location of object stimuli. What is the neural basis that gives rise to these findings?

Neural model

We saw a weak clustering of space-sensitive and space-insensitive voxels within an object-selective area, and space-sensitive voxels were generally distributed throughout the ROIs. It

seems likely that this distribution of voxels reflects a similar underlying distribution of "space-sensitive" and "category-sensitive" neurons. The two types of neurons might be distributed throughout object-selective areas, with some degree of clustering according to their stimulus preferences. Nearby neurons in the inferior temporal cortex of monkeys tend to share the same stimulus preferences (Tamura, Kaneko, & Fujita, 2005), and a such clustering of functionally similar neurons might give rise to the "category-sensitive" and "space-sensitive" voxels in our study.

"Space-sensitive" and "category-sensitive" here means that neurons are either more space-sensitive than they are category-sensitive, or that they are more category-sensitive than they are space-sensitive (see the model in **Figure 3.12**). Thus, all visual neurons in FFA and PPA encode both category and space, but the extent of coding one of the two aspects comes at the expense of coding the other aspect. If a neuron is, for example, highly sensitive to space, it consequently has less potential to discriminate between object categories. This explains why our space-sensitive voxels exhibited category selectivity, but to a lesser extent than the space-insensitive voxels. In contrast, a neuron that is highly sensitive to object category is only weakly sensitive to space and does not fulfill our criteria for "space sensitivity".

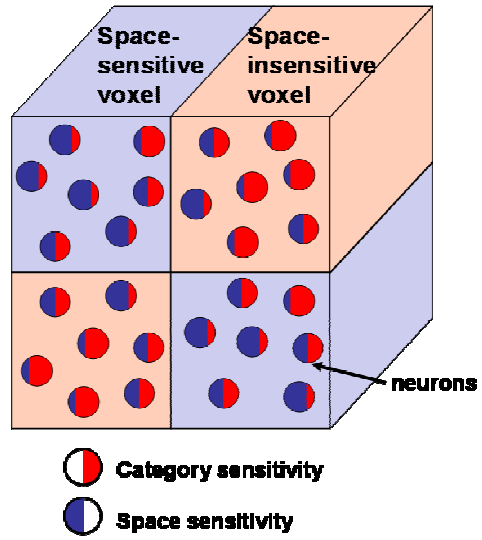

Figure 3.12: **Model of the neural representation of space and category in object-selective areas. The cube includes four voxels, of which two are space-sensitive (in light blue) and two are space-insensitive (light red). Each voxel contains neurons (represented by circles) with varying degrees of category selectivity and space sensitivity. The extent of category selectivity is indicated by a red filling, the extent of space sensitivity is indicated by blue filling. Every neuron in this model is both category-selective and space-sensitive, but there is a trade-off between the two. More space-sensitive neurons are less category-selective, while more category-selective neurons are less space-sensitive. Neurons with similar degrees of category or space representation are distributed throughout object-selective areas, but they show some extent of clustering. This weak clustering gives rise to the net behavior of a voxel to be either space-sensitive or space-insensitive.**

4 General Discussion

The experiments described in this thesis address the question of how category and space are represented in the brain. In particular, we asked whether object category is encoded in specialized modules or whether it is distributed throughout the ventral stream. Furthermore, we investigated the extent of space representation in ventral stream areas.

Evidence for a distributed representation of category

In chapter 2 we tested two opposing theories on the encoding of category. One theory assumes that category is represented in specialized modules (Kanwisher et al., 1997), while the other theories suggests that category information is distributed throughout the ventral stream (Ishai et al., 1999). We conducted an fMRI-A experiment and tested whether ventral stream areas exhibit adaptation only to their preferred categories or also to non-preferred categories. If the first theory were correct and ventral stream areas encode exclusively their preferred category, then they should show adaptation only to their preferred category. If, on the other hand, the second theory is correct and these areas also encode some properties of non-preferred categories, then adaptation should occur across object categories, but to a lesser extent for non-preferred categories. We found that ventral stream areas adapted to both preferred and non-preferred object stimuli, and the magnitude of the adaptation effect was higher for preferred categories.

A study similar to ours has been published recently. Weiner et al. (Weiner et al., 2010) also investigated category selectivity by comparing adaptation profiles in a block and an event-related design. The authors also found adaptation in ventral stream regions across categories. Adaptation in face- and limb-selective regions was stronger for preferred than for non-preferred categories in

both block and event-related designs, while the house-selective region showed a dissociation of adaptation profiles. Specifically, this region also exhibited the strongest adaptation for its preferred category in the block design, but in the event-related design the strongest adaptation occurred for non-preferred categories. This dissociation in the house-selective region is in contrast to our findings, as we found the same tendency for stronger adaptation to preferred categories in both designs, albeit not significant in the event-related design. The study of Weiner et al. differed from ours, however, with respect to the event-related timing parameters. The authors were interested in the influence of timing between stimulus repetitions on the adaptation profiles across the ventral stream. Hence, their block design consisted of novel or repeated stimuli that immediately followed each other, while in their event-related design repeated stimuli were separated by on average 20 trials. The authors proposed that different time scales of stimulus repetition affect lateral (face- and limb-selective) and medial (house-selective) ventral stream regions differently and should therefore be taken into account when planning fMRI studies. The purpose of our study, in contrast, was to detect any potential differences in block and event-related designs with respect to attentional factors. Thus, our designs did not differ in the temporal separation of repeated stimuli, but instead differed only in the predictability of stimuli. We did not find that predictability had a large impact on the adaptation profiles in FFA and PPA. A study on the word-frequency effect (Chee, Venkatraman, Westphal, & Siong, 2003) similarly compared the two types of fMRI designs and found no differences.

As mentioned above, our study favors the theory of a distributed processing of object information and undermines the notion of modules that exclusively encode one category. But of what nature is this distributed information? Could it be low-level features such as spatial frequency? Also Ishai et al. (Ishai et al., 1999) suggested that information about the object

category is present throughout the ventral temporal cortex, but that some areas, namely FFA, PPA and other areas that respond preferentially to one category, are clusters of information characteristics that are mainly shared within a category but not between categories. Such a description would fit to spatial frequency as the information in question, because faces, houses and objects have characteristic spatial frequency spectra, which are more similar in different exemplars of one category than in exemplars of different categories. However, spatial frequency is an unlikely candidate for an organizational principle of the ventral stream, because in our experiment we controlled for differences in the spatial frequency spectrum of face and house pictures. If FFA and PPA responded preferentially to the characteristic spatial frequency spectra of faces and houses, then our data should have yielded the same amount of adaptation for the preferred and non-preferred categories. Instead, we found stronger adaptation for the preferred category than for the non-preferred category. Thus, there must be another informational aspect about category. Also Ishai et al. (Ishai et al., 1999) excluded the possibility of low-level features such as spatial frequency or texture to carry the crucial information on category. They hypothesize that object shape primitives might be the content of the distributed information. This question is still unanswered and remains an open topic for future investigations.

Space is a dimension in the ventral stream

In chapter 3 we presented a new way of investigating the representation of space in ventral stream areas. We combined retinotopic mapping techniques with the presentation of object stimuli and applied a ROI-based analysis. We were able to demonstrate that the ventral stream areas FFA and PPA are highly space-sensitive and that the representation of space covers nearly the entire visual field. Furthermore, we have shown that the encoding of category and the encoding of space partially interact, because we found indications that spatial sensitivity is

highest for the preferred category. Our study sheds new light on the functional properties of the ventral stream, because it can no longer be assumed that ventral stream areas have the sole purpose of processing the identity of objects. Rather, these areas compute both the identity and location of objects. It appears that the dimensions of category and space co-exist in the same voxels, perhaps even in the same neurons. We found voxels that showed preference for a specific category, as well as for a specific spatial location of stimuli. Furthermore, voxels that were more robustly sensitive to space were at the same time less sensitive to category membership. This fact might be important for the interpretation of studies that have investigated or will investigate ventral stream regions by averaging the signal of all voxels in a given ROI. For example, it is not surprising that many previous studies on the representation of space, which generally employed averaged analyses, have not found spatial sensitivity in ventral stream regions, because voxels that are mainly category-sensitive might have overpowered the signal of more space-sensitive voxels. Furthermore, these studies collapse the signal across voxels which we have shown to represent different locations, and consequently cannot detect any spatial preference.

In conclusion, in this thesis we have investigated two hypothesized dimensions of the ventral stream: category and space. We have shown that category is not encoded by modules that exclusively represent one category. Rather, information about category is distributed throughout ventral stream regions and is clustered in areas that respond maximally to certain categories. Similarly, space is represented throughout the ventral stream and co-exists with the representation of category. These findings enhance our knowledge about how information is represented in the brain by showing that information processing is more widespread than formerly thought. Our studies also show that fMRI techniques like fMRI-A and voxel-based

analyses can reveal brain mechanisms to more detail than conventional signal averaging analyses and are therefore important tools for future research in cognitive neuroscience.

5 Appendix

Table 5.1: Talairach coordinates of FFA and PPA as defined in the separate object localizer (experiment 2).

Subject	ROI	x	y	z	nr of voxels (voxel size: 1mm³)
S1	FFA right	34	-48	-13	2271
	left	-37	-59	-10	924
	PPA right	23	-44	-7	4062
	left	-28	-45	-10	2528
S2	FFA right	38	-53	-9	2113
	left	-42	-49	-11	1179
	PPA right	25	-53	-8	3795
	left	-26	-53	-5	1864
S3	FFA right	42	-43	-17	555
	left	-34	-38	-20	619
	PPA right	26	-41	-8	449
	left	-23	-40	-9	516
S4	FFA right	33	-57	-14	1548
	left	-39	-65	-13	971
	PPA right	25	-48	-7	718
	left	-25	-39	-9	408
S5	FFA right	33	-44	-14	814
	left	-36	-40	-19	792
	PPA right	25	-30	-11	1326
	left	-25	-34	-14	1480
S6	FFA right	36	-44	-20	2004
	left	-33	-41	-18	1001
	PPA right	21	-44	-8	5382
	left	-24	-38	-12	3363
S7	FFA right	35	-40	-16	734
	left	-36	-38	-14	732
	PPA right	27	-41	-9	1685
	left	-28	-41	-7	1360
S8	FFA right	43	-43	-11	551
	left	-40	-53	-15	160
	PPA right	30	-43	-3	370
	left	-26	-41	-7	552

Figure 5.1: **Spatial sensitivity maps of subjects 2 to 8 (experiment 2).**

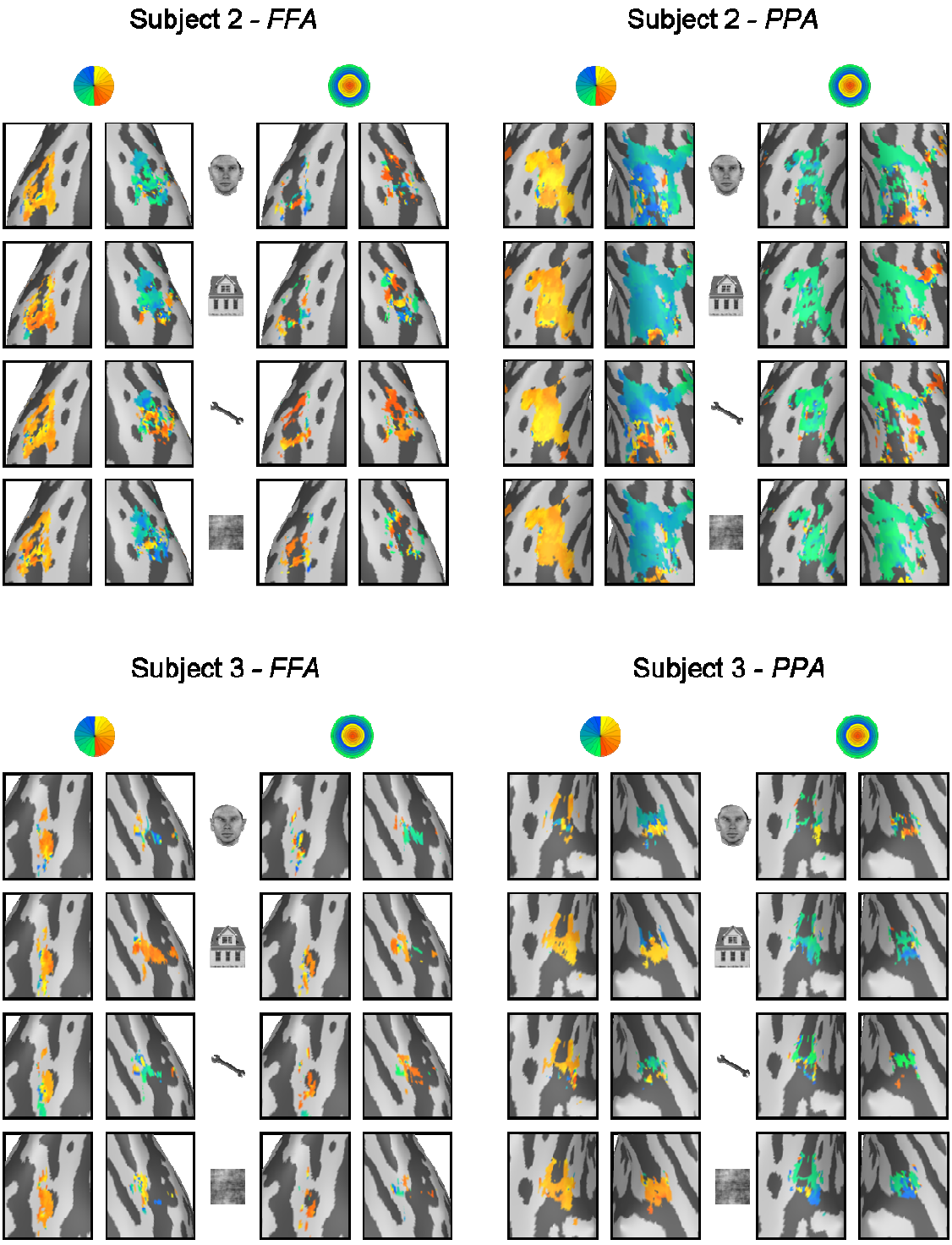

Subject 4 - *FFA*

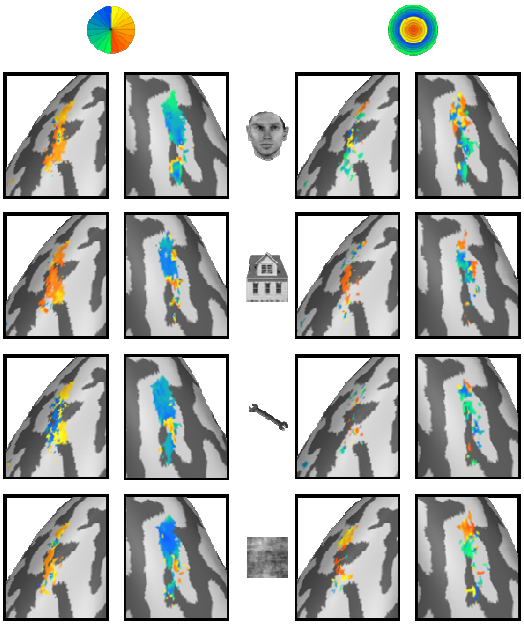

Subject 4 - *PPA*

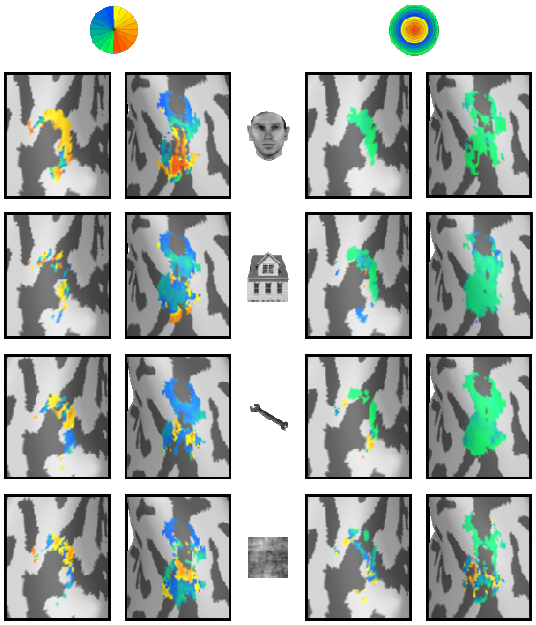

Subject 5 - *FFA*

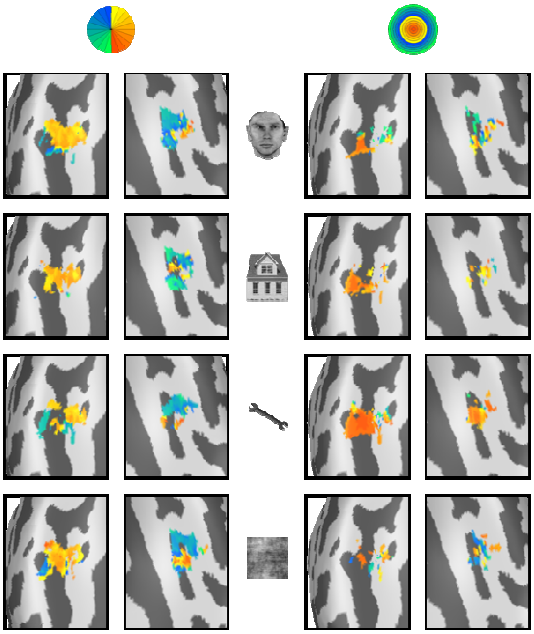

Subject 5 - *PPA*

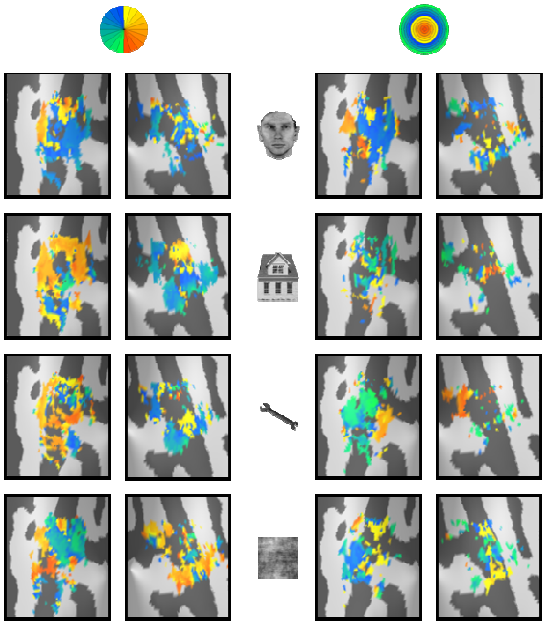

Subject 6 - *FFA*

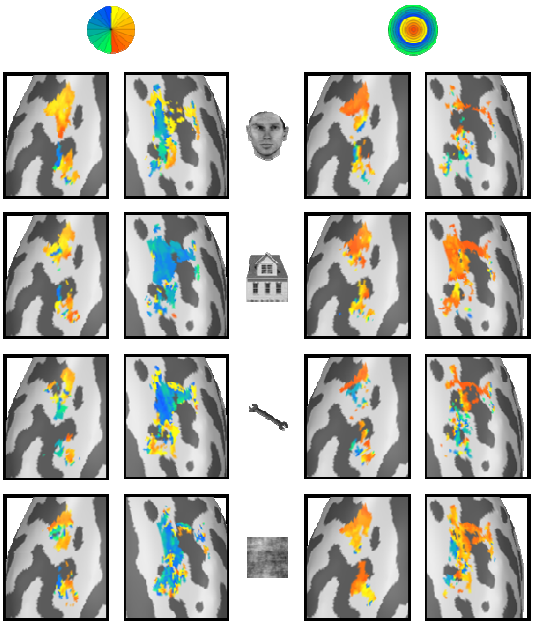

Subject 6 - *PPA*

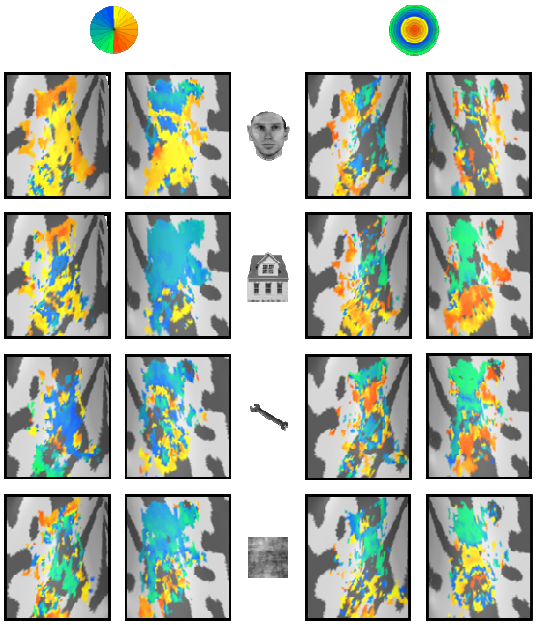

Subject 7 - *FFA*

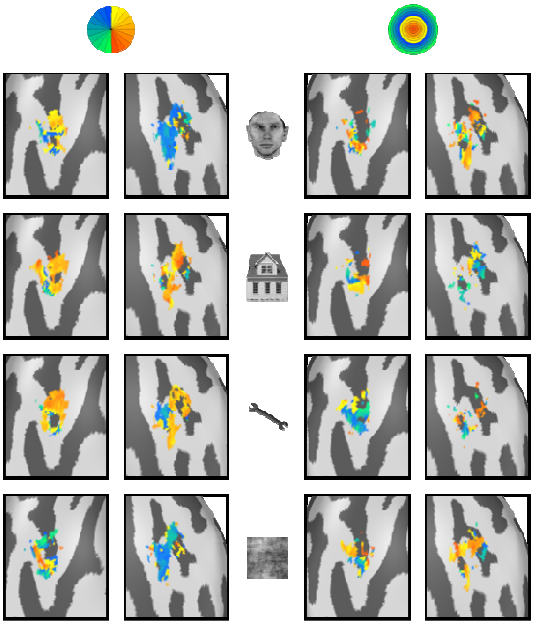

Subject 7 - *PPA*

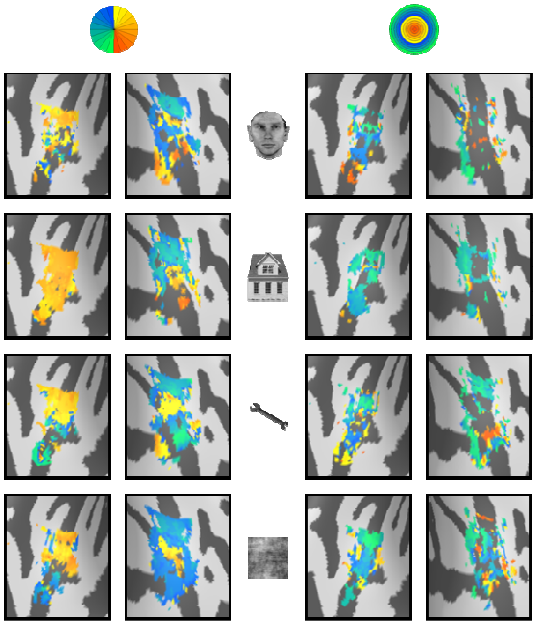

Subject 8 - *FFA*

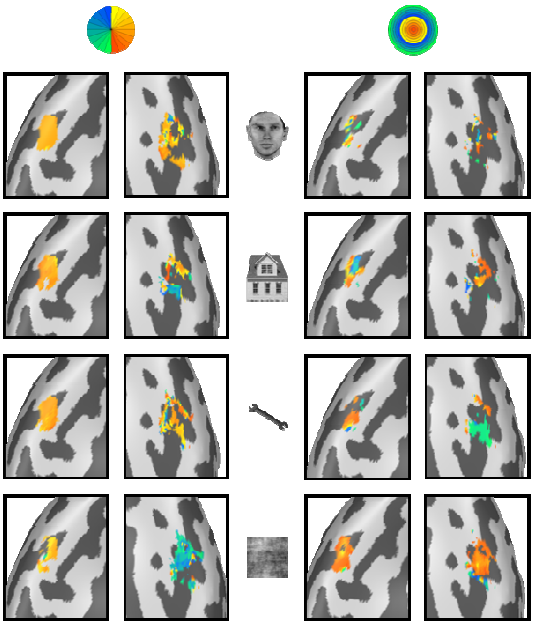

Subject 8 - *PPA*

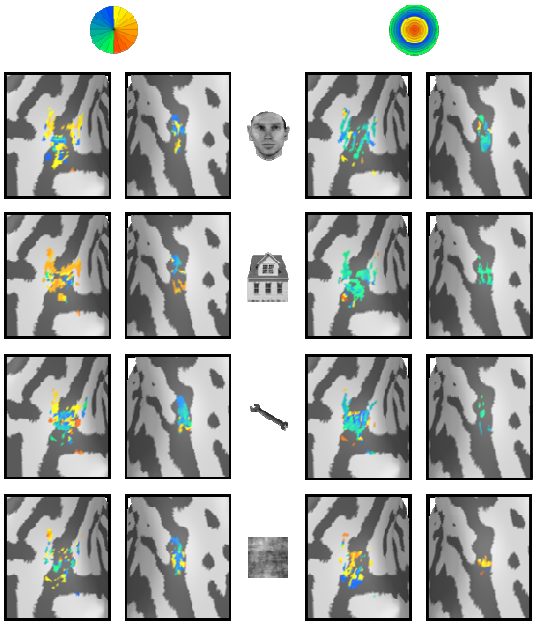

6 References

Aguirre, G. K., Zarahn, E., & D Esposito, M. (1998). An Area within Human Ventral Cortex Sensitive to Building Stimuli: Evidence and Implications. *Neuron, 21*(2), 373-383.

Arcaro, M. J., McMains, S. A., Singer, B. D., & Kastner, S. (2009). Retinotopic Organization of Human Ventral Visual Cortex. *The Journal of Neuroscience, 29*(34), 10638-10652.

Avidan, G., Hasson, U., Hendler, T., Zohary, E., & Malach, R. (2002). Analysis of the Neuronal Selectivity Underlying Low fMRI Signals. *Current biology : CB, 12*(12), 964-972.

Bartels, A., Logothetis, N. K., & Moutoussis, K. (2008). fMRI and its interpretations: an illustration on directional selectivity in area V5/MT. *Trends in Neurosciences, 31*(9), 444-453.

Behrmann, M., & Avidan, G. (2005). Congenital prosopagnosia: face-blind from birth. *Trends in Cognitive Sciences, 9*(4), 180-187.

Bindemann, M., Scheepers, C., & Burton, M. A. (2009). Viewpoint and center of gravity affect eye movements to human faces. *Journal of Vision, 9*(2), 1-16.

Brainard, D. H. (1997). The Psychophysics Toolbox. *Spatial Vision, 10*, 433-436.

Busigny, T., Graf, M., Mayer, E., & Rossion, B. (2010). Acquired prosopagnosia as a face-specific disorder: Ruling out the general visual similarity account. *Neuropsychologia, 48*(7), 2051-2067.

Cavina-Pratesi, C., Kentridge, R. W., Heywood, C. A., & Milner, A. D. (2010). Separate Channels for Processing Form, Texture, and Color: Evidence from fMRI Adaptation and Visual Object Agnosia. *Cerebral Cortex, 20*(10), 2319-2332.

Chao, L. L., Haxby, J. V., & Martin, A. (1999). Attribute-based neural substrates in temporal cortex for perceiving and knowing about objects. *Nat Neurosci, 2*(10), 913-919.

Chee, M. W., Venkatraman, V., Westphal, C., & Siong, S. C. (2003). Comparison of block and event-related fMRI designs in evaluating the word-frequency effect. *Human Brain Mapping, 18*(3), 186-193.

Daniel, P. M., & Whitteridge, D. (1961). The representation of the visual field on the cerebral cortex in monkeys. *The Journal of Physiology, 159*(2), 203-221.

Downing, P. E., Chan, A. W. Y., Peelen, M. V., Dodds, C. M., & Kanwisher, N. (2006a). Domain Specificity in Visual Cortex. *Cerebral Cortex, 16*(10), 1453-1461.

Downing, P. E., Chan, A. W. Y., Peelen, M. V., Dodds, C. M., & Kanwisher, N. (2006b). Domain Specificity in Visual Cortex. *Cerebral Cortex, 16*, 1453-1461.

Dumoulin, S. O., & Wandell, B. A. (2008). Population receptive field estimates in human visual cortex. *NeuroImage, 39*, 647–660.

Engel, S. A., Rumelhart, D. E., Wandell, B. A., Lee, A. T., Glover, G. H., Chichilnisky, E.-J., et al. (1994). fMRI of human visual cortex. *Nature, 369*(6481), 525-525.

Epstein, R., Graham, K. S., & Downing, P. E. (2003). Viewpoint-Specific Scene Representations in Human Parahippocampal Cortex. *Neuron, 37*(5), 865-876.

Epstein, R., Harris, A., Stanley, D., & Kanwisher, N. (1999). The Parahippocampal Place Area: Recognition, Navigation, or Encoding? *Neuron, 23*(1), 115-125.

Epstein, R., & Kanwisher, N. (1998). A cortical representation of the local visual environment. *Nature, 392*(6676), 598-601.

Ewbank, M. P., Schluppeck, D., & Andrews, T. J. (2005). fMR-adaptation reveals a distributed representation of inanimate objects and places in human visual cortex. *NeuroImage, 28*(1), 268-279.

Fang, F., Murray, S. O., Kersten, D., & He, S. (2005). Orientation-Tuned fMRI Adaptation in Human Visual Cortex. *J Neurophysiol, 94*(6), 4188-4195.

Friston, K. J., Zarahn, E., Josephs, O., Henson, R. N. A., & Dale, A. M. (1999). Stochastic Designs in Event-Related fMRI. *NeuroImage, 10*(5), 607-619.

Gauthier, I. (2000). What constrains the organization of the ventral temporal cortex? *Trends in Cognitive Sciences, 4*(1), 1-2.

Gauthier, I., Tarr, M. J., Andersen, A. W., Skudlarski, P., & Gore, J. C. (1999). Activation of the middle fusiform 'face area' increases with expertise in recognizing novel objects. *Nature Neuroscience, 2*, 568-573.

Genovese, C. R., Lazar, N. A., & Nichols, T. (2002). Thresholding of Statistical Maps in Functional Neuroimaging Using the False Discovery Rate. *NeuroImage, 15*(4), 870-878.

Goebel, R., Esposito, F., & Formisano, E. (2006). Analysis of functional image analysis contest (FIAC) data with brainvoyager QX: From single-subject to cortically aligned group general linear model analysis and self-organizing group independent component analysis. *Human Brain Mapping, 27*(5), 392-401.

Grill-Spector, K. (2003). The neural basis of object perception. *Current Opinion in Neurobiology, 13*(2), 159-166.

Grill-Spector, K., & Malach, R. (2001). fMR-adaptation: a tool for studying the functional properties of human cortical neurons. *Acta Psychologica, 107*(1-3), 293-321.

Grill-Spector, K., & Malach, R. (2004). THE HUMAN VISUAL CORTEX. *Annual Review of Neuroscience, 27*(1), 649-677.

Hasson, U., Levy, I., Behrmann, M., Hendler, T., & Malach, R. (2002). Eccentricity Bias as an Organizing Principle for Human High-Order Object Areas. *Neuron, 34*(3), 479-490.

Haxby, J. V., Gobbini, M. I., Furey, M. L., Ishai, A., Schouten, J. L., & Pietrini, P. (2001). Distributed and Overlapping Representations of Faces and Objects in Ventral Temporal Cortex. *Science, 293*, 2425-2430.

Heilman, K. M., & Abell, T. V. D. (1980). Right hemisphere dominance for attention. *Neurology, 30*(3), 327.

Hemond, C. C., Kanwisher, N. G., & Op de Beeck, H. P. (2007). A Preference for Contralateral Stimuli in Human Object- and Face-Selective Cortex. *PLoS ONE, 2*(6), e574.

Hubel, D. H., & Wiesel, T. N. (1968). Receptive fields and functional architecture of monkey striate cortex. *The Journal of Physiology, 195*, 215-243.

Ishai, A., Ungerleider, L. G., Martin, A., Schouten, J. L., & Haxby, J. V. (1999). Distributed representation of objects in the human ventral visual pathway. *Proceedings of the National Academy of Sciences of the United States of America, 96*(16), 9379-9384.

Kanwisher, N. (2000). Domain specificity in face perception. *Nature Neuroscience, 3*(8), 759-762.

Kanwisher, N., McDermott, J., & Chun, M. M. (1997). The Fusiform Face Area: A Module in Human Extrastriate Cortex Specialized for Face Perception. *The Journal of Neuroscience, 17*, 4302-4311.

Kanwisher, N., & Yovel, G. (2006). The Fusiform Face Area: A Cortical Region Specialized for the Perception of Faces. *Philosophical Transactions of the Royal Society of London B, 361*, 2109-2128.

Kaul, C., Bahrami, B., & Rees, G. (2009). Multivoxel fMRI analysis reveals the representation of spatial frequency information in human primary visual cortex. *Journal of Vision, 9*(8), 766.

Konen, C. S., & Kastner, S. (2008). Two hierarchically organized neural systems for object information in human visual cortex. *Nat Neurosci, 11*(2), 224-231.

Kovács, G., Cziraki, C., Vidnyánszky, Z., Schweinberger, S. R., & Greenlee, M. W. (2008). Position-specific and position-invariant face aftereffects reflect the adaptation of different cortical areas. *NeuroImage, 43*, 156–164.

Kravitz, D. J., Kriegeskorte, N., & Baker, C. I. (2010). High-Level Visual Object Representations Are Constrained by Position. *Cerebral Cortex, doi: 10.1093/cercor/bhq042*.

Krekelberg, B., Boynton, G. M., & van Wezel, R. J. A. (2006). Adaptation: from single cells to BOLD signals. *Trends in Neurosciences, 29*(5), 250-256.

Logothetis, N. K. (2008). What we can do and what we cannot do with fMRI. *Nature, 453*(7197), 869-878.

Mahon, B., Anzelotti, S., Schwarzbach, J., Zampini, M., & Caramazza, A. (2009). Category-Specific Organization in the Human Brain Does Not Require Visual Experience. *Neuron, 63*, 397–405.

Malach, R., Reppas, J. B., Benson, R. R., Kwong, K. K., Jiang, H., Kennedy, W. A., et al. (1995). Object-related activity revealed by functional magnetic resonance imaging in human occipital cortex. *Proceedings of the National Academy of Sciences of the United States of America, 92*(18), 8135-8139.

Maunsell, J. H. R., & Newsome, W. T. (1987). Visual Processing in Monkey Extrastriate Cortex. *Annual Review of Neuroscience, 10*(1), 363-401.

McCarthy, G., Puce, A., Gore, J. C., & Allison, T. (1997). Face-Specific Processing in the Human Fusiform Gyrus. *Journal of Cognitive Neuroscience, 9*(5), 605-610.

Mesulam, M. M. (1999). Spatial attention and neglect: parietal, frontal and cingulate contributions to the mental representation and attentional targeting of salient extrapersonal events. *Philosophical Transactions of the Royal Society of London. Series B: Biological Sciences, 354*(1387), 1325-1346.

Milner, A. D., Dijkerman, H. C., McIntosh, R. D., Rossetti, Y., Pisella, L., & C. Prablanc, D. P. Y. R. (2003). Delayed reaching and grasping in patients with optic ataxia. In *Progress in Brain Research* (Vol. Volume 142, pp. 225-242): Elsevier.

Moscovitch, M., Winocur, G., & Behrmann, A. (1997). What Is Special about Face Recognition?: Nineteen Experiments on a Person with Visual Object Agnosia and Dyslexia but Normal Face Recognition. *J. Cogn. Neurosci., 9*(5), 555-604.

Mur, M., Ruff, D. A., Bodurka, J., Bandettini, P. A., & Kriegeskorte, N. (2010). Face-Identity Change Activation Outside the Face System: "Release from Adaptation" May Not Always Indicate Neuronal Selectivity. *Cerebral Cortex, 20*(9), 2027-2042.

Op de Beeck, H. P., Haushofer, J., & Kanwisher, N. G. (2008). Interpreting fMRI data: maps, modules and dimensions. *Nat Rev Neurosci, 9*(2), 123-135.

Pelli, D. G. (1997). The VideoToolbox software for visual psychophysics: transforming numbers into movies. *Spatial Vision, 10*, 437-442.

Pilgrim, L. K., Fadili, J., Fletcher, P., & Tyler, L. K. (2002). Overcoming Confounds of Stimulus Blocking: An Event-Related fMRI Design of Semantic Processing. *NeuroImage, 16*(3, Part 1), 713-723.

Pourtois, G., Schwartz, S., Spiridon, M., Martuzzi, R., & Vuilleumier, P. (2009). Object Representations for Multiple Visual Categories Overlap in Lateral Occipital and Medial Fusiform Cortex. *Cerebral Cortex, 19*(8), 1806-1819.

Puce, A., Allison, T., Gore, J. C., & McCarthy, G. (1995). Face-sensitive regions in human extrastriate cortex studied by functional MRI. *J Neurophysiol, 74*(3), 1192-1199.

Sayres, R., & Grill-Spector, K. (2008). Relating Retinotopic and Object-Selective Responses in Human Lateral Occipital Cortex. *Journal of Neurophysiology, 100*, 249–267.

Schwarzbach, J. (submitted). A Simple Framework (ASF) for behavioral and neuroimaging experiments based on the Psychophysics Toolbox for Matlab.

Schwarzlose, R. F., Swisher, J. D., Dang, S., & Kanwisher, N. (2008). The distribution of category and location information across object-selective regions in human visual cortex. *Proceedings of the National Academy of Science, 105*(11), 4447–4452.

Serences, J., Schwarzbach, J., Courtney, S., Golay, X., & Yantis, S. (2004). Control of object-based attention in human cortex. *Cerebral Cortex, 14*(12), 1346-1357.

Sereno, M. I., Dale, A. M., Reppas, J. B., Kwong, K. K., Belliveau, J. W., Brady, T. J., et al. (1995). Borders of multiple visual areas in humans revealed by functional magnetic resonance imaging. *Science, 268*(5212), 889-893.

Shmuelof, L., & Zohary, E. (2005). Dissociation between Ventral and Dorsal fMRI Activation during Object and Action Recognition. *Neuron, 47*(3), 457-470.

Smith, A. T., Singh, K. D., Williams, A. L., & Greenlee, M. W. (2001). Estimating Receptive Field Size from fMRI Data in Human Striate and Extrastriate Visual Cortex. *Cerebral Cortex, 11*(12), 1182-1190.

Talairach, J., & Tournoux, P. (1988). *Co-planar Stereotaxic Atlas of the Human Brain. 3-dimensional Proportional System: An Approach to Cerebral Imaging*: Thieme Medical Publishers, New York.

Tamura, H., Kaneko, H., & Fujita, I. (2005). Quantitative analysis of functional clustering of neurons in the macaque inferior temporal cortex. *Neuroscience Research, 52*(4), 311-322.

Tootell, R. B., Mendola, J. D., Hadjikhani, N. K., Liu, A. K., & Dale, A. M. (1998). The representation of the ipsilateral visual field in human cerebral cortex. *Proceedings of the national academy of science, 95*(3), 818-824.

Tootell, R. B., Silverman, M. S., & De Valois, R. L. (1981). Spatial frequency columns in primary visual cortex. *Science, 214*(4522), 813-815.

Tsao, D. Y., & Livingstone, M. S. (2008). Mechanisms of Face Perception. *Annual Review of Neuroscience, 31*(1), 411-437.

Ungerleider, L. G., Mishkin, M., Ingle, D. J., Goodale, M., & Mansfield, R. J. W. (1982). Two Cortical Visual Systems. In *Analysis of Visual Behaviour* (pp. 549-586).

Wandell, B. A., Dumoulin, S. O., & Brewer, A. A. (2007). Visual Field Maps in Human Cortex. *Neuron, 56*, 366-383.

Weiner, K. S., Sayres, R., Vinberg, J., & Grill-Spector, K. (2010). fMRI-adaptation and category selectivity in human ventral temporal cortex: Regional differences across time scales. *J Neurophysiol*, jn.01108.02009.

Yovel, G., & Kanwisher, N. (2005). The FFA shows a face inversion effect that is correlated with the behavioral face inversion effect. *Journal of Vision, 5*(8), 632.